AD-A045 814 MAXWELL LABS INC SAN DIEGO CALIF F/G 9/1
HIGH POWER SPARK GAP OPTIMIZATION.(U)
JUN 77
UNCLASSIFIED MLR-670 N60921-76-C-0274
NL

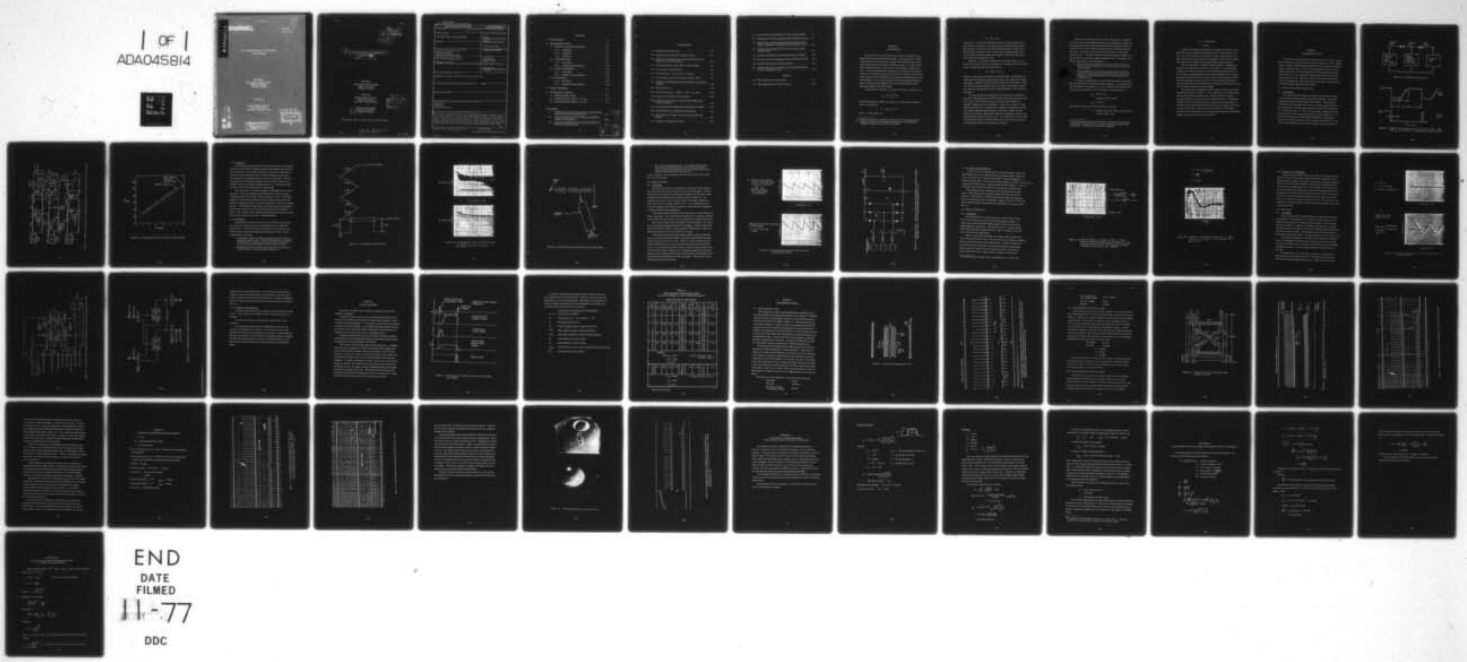

END
DATE FILMED
11-77
DDC

MAXWELL

MLR-670

June 16, 1977

HIGH POWER SPARK GAP OPTIMIZATION
FINAL REPORT

Submitted to

Naval Surface Weapons Center
Dahlgren Laboratory
Dahlgren, Virginia

Prepared By

Maxwell Laboratories, Inc.
9244 Balboa Avenue
San Diego, California 92123

(14) MLR-670

(11) 16 June 1977

(12) 55 p.

(6) HIGH POWER SPARK GAP OPTIMIZATION •

(7) FINAL REPORT.

Submitted to

Naval Surface Weapons Center
Dahlgren Laboratory
Dahlgren, Virginia

Prepared by

Maxwell Laboratories, Inc.
9244 Balboa Avenue
San Diego, California 92123

Under Contract Number
(15) N6ø921-76-C-ø274

Approved for public release; distribution unlimited.

UNCLASSIFIED

SECURITY CLASSIFICATION OF THIS PAGE *(When Data Entered)*

REPORT DOCUMENTATION PAGE		READ INSTRUCTIONS BEFORE COMPLETING FORM
1. REPORT NUMBER	2. GOVT ACCESSION NO.	3. RECIPIENT'S CATALOG NUMBER
4. TITLE *(and Subtitle)* HIGH POWER SPARK GAP OPTIMIZATION		5. TYPE OF REPORT & PERIOD COVERED Final
		6. PERFORMING ORG. REPORT NUMBER MLR-670
7. AUTHOR(s)		8. CONTRACT OR GRANT NUMBER(s) N-60921-76-C-0274 New
9. PERFORMING ORGANIZATION NAME AND ADDRESS Maxwell Laboratories, Inc. 9244 Balboa Avenue San Diego, California 92123		10. PROGRAM ELEMENT, PROJECT, TASK AREA & WORK UNIT NUMBERS
11. CONTROLLING OFFICE NAME AND ADDRESS Naval Surface Weapons Center Dahlgren, Va. 22448		12. REPORT DATE 16 June 1977 13. NUMBER OF PAGES 53
14. MONITORING AGENCY NAME & ADDRESS*(if different from Controlling Office)*		15. SECURITY CLASS. *(of this report)* Unclassified 15a. DECLASSIFICATION/DOWNGRADING SCHEDULE

16. DISTRIBUTION STATEMENT *(of this Report)*

Approved for public release; distribution unlimited.

17. DISTRIBUTION STATEMENT *(of the abstract entered in Block 20, if diffe... Report)*

18. SUPPLEMENTARY NOTES

19. KEY WORDS *(Continue on reverse side if necessary and identify by block number)*

High Power
Spark Gap
Switch Performance

20. ABSTRACT *(Continue on reverse side if necessary and identify by block number)*

This report completes the High Power Spark Gap Optimization program, which was begun under a previous contract with Wright-Patterson AFB. In that program, data was obtained in the power range of 1-5 MW to investigate switch performance at rep-rates up to 500 pps, and at voltages up to 60 kV. In the current program, the main experimental objectives were to demonstrate spark gap power above 5 MW per switch, and raise operating voltage into the 100 kV range.

DD FORM 1 JAN 73 1473 EDITION OF 1 NOV 65 IS OBSOLETE
S/N 0102-LF-014-6601

UNCLASSIFIED

SECURITY CLASSIFICATION OF THIS PAGE *(When Data Entered)*

CONTENTS

ILLUSTRATIONS

TABLES

SECTION 1

INTRODUCTION

Maxwell Laboratories presents this final report in completion of the High Power Spark Gap Optimization program. This program was, in effect, a continuation of one started under a contract with Wright-Patterson AFB.[1] In that program, data was obtained in the power range of 1 - 5 MW to investigate switch performance at rep-rates up to 500 pps and at voltages up to 60 kV. For the maximum power experiments, two switches were connected in parallel to reduce the power delivered per switch to about 2.7 MW to maintain minimum pre-fire probability and to demonstrate the feasibility of paralleling switches. In the current program, the main experimental objectives were to demonstrate spark gap power above 5 MW per switch and raise operating voltage into the 100 kV range.

The actual power dissipated in a resistive load due to a pulse train is:

$$P_a = \text{prf} \times \int_0^T IV\,dt$$

where the integration is taken over one period. If the voltage waveshape is square, the equation is

$$P = \text{prf} \times V \times I \times \tau$$

where τ is pulse width, or,

---

[1] MLR-484, May 1975. High Power Spark Gap Switch Development, submitted to Air Force Aero Propulsion Laboratory, Air Force Systems Command, Wright-Patterson AFB, Ohio 48433.

$$P = \text{prf} \times V \times Q$$

where $Q = I\tau$. The switch transmitting this power to a load consumes only a small fraction of that power. The objective of the simulation facility used in this program is to create the conditions in the switch known to effect switch recovery-after-breakdown. Thus, the same peak voltage amplitude, peak current, and total charge transfer are created in the switch as if the switch were operated in a high power circuit.

Therefore, if a switch can reliably hold-off the peak voltage V_o, discharge with the peak current I_o and charge Q_o, at the rep rate, prf, the power which it is effectively delivering to the load is:

$$P_s = \text{prf} \times V_o \times I_o \times \tau$$

where P_s is the power indicated and τ is the pulse width. In this report, we approximate $I\tau$ with Q_o the charge initially stored in the capacitor the switch discharges. Appendix I contains additional discussion on this matter. There, it is shown the energy dissipated by the switch gas in the simulator exceeds that expected in the high power circuit, lending credibility to this simulation technique.

The above calculation of simulated power is based on the assumption the actual voltage applied to the switch equals that delivered to the load in the real circuit. This is strictly true only in pulsers whose impedance is negligible compared to the load impedance. Other types, such as line-type pulsers and PFN's, have a characteristic impedance comparable to the load. If the pulser impedance equals the load, in a PFN for example, the load voltage is one-half the applied switch voltage and consequently, the power the switch actually controls is $(1/2)V_o\ Q_o$ prf. For consistency with other recent literature in this field, this report assumes full switch voltage is delivered to the load and, therefore, switch power is $(\text{prf})V_oQ_o$.

This program included tests on two switch configurations. Configuration I was similar to that employed during the previous program and provided a data base with which to compare facility and switch operation with that obtained previously. The second configuration was an improved design, with provisions to efficiently sweep the arc region by means of a more highly directed air flow. The latter configuration was found capable of higher voltage and power, and operated reliably at reduced air flow. In summary, the program achievements were the following:

1. Reliable and continuous operation at 90 kV to 100 kV with low restrike and no-fire probabilities at a 250 pps rep rate and 240 mC charge transfer.
2. Drastic reduction of flow-rate requirements from ≃ 150 SCFM[1] required for the first gap design (Configuration I) to 60 SCFM per switch at ≈ 5.5 MW simulated power for the second gap design (Configuration II).

To compare simulated power to actual power delivered to the load during these experiments, the charge transfer is required. At maximum power, a 30 μF capacitor was charged to V_s = 8 kV to provide 240 mC charge transfer and the peak current of 4.5 kA. Therefore, simulated power is:

$$P_s = \text{prf} \times V \times Q$$

$$= 250 \text{ pps} \times 90 \text{ kV} \times 240 \text{ mC}$$

$$P_s = 5.4 \text{ MW}$$

Actual power is the product of stored energy and rep rate.

$$P_a = 250 \text{ pps} \times 1/2\ CV_s^2$$ where V_s is high-power source voltage = 8 kV.

---

[1] 150 SCFM (standard cubic feet per minute) corresponds to a flow velocity of 3300 ft per minute in the 2-7/8" diameter output tubing used in these experiments. 1 SCFM is 31 grams/minute mass flow.

$$P_a = 250 \text{ pps} \times 960 \text{ J}$$

$$= 240 \text{ kW}.$$

To date, the maximum simulated power was about 5.4 MW per switch. This level occurred repeatably and reliably at 90 kV. Operation above that power level caused reliability problems due to high-voltage tracking in the output transformer of the voltage waveform generator (VWG) but the switches under test appeared capable of handling still higher voltage and power.

The test configuration employed during this program is fundamentally the same as that described in reference 1 (MLR-484). To accomplish the simulation, two identical switches are incorporated in the high-current circuit to enable an independent high-voltage, high-impedance source to charge the common-point between the switches in order to test their ability to withstand rep-rated high-voltage waveforms. As described in the following report, several microhenries of inductance are introduced into this high-current circuit to attain the desired output waveshape.

The double-switch configuration and the inductive isolation are required to enable the simulator to operate. In actual high-power-circuit applications only one switch would be required with virtually no inductive isolation, assuming the switch can be operated in its self-break mode. If triggering is required, in a PFN circuit for example, a small series inductance may be required to permit closure by delivering a fast rise time trigger pulse to one of the switch electrodes. The relatively high impedance of this trigger generator and the short duration of the trigger pulse would prevent observable trigger current from flowing in the output load.

SECTION 2
EXPERIMENTAL SETUP

This section describes the main components in the test circuit. A summary of calibration and a description of the circuit operation is also included. Figure 2-1 shows a simplified diagram of the circuit and Figure 2-2 indicates timing of the main events. Figure 2-3 shows the entire circuit in its most recent configuration. The latter figure has the voltage waveform generator (VWG) shown in (a), the current circuit (high-power source) in (b) and the trigger generator in (c). Reference 1 (MLR-484) provides a detailed description of the apparatus. The intention here is to summarize the test setup and include changes made during this program.

2.1 VOLTAGE WAVEFORM GENERATOR

2.1.1 Description

The voltage waveform generator provides the high-voltage waveform to the common point between the test and isolation switches. During this program the maximum output voltage is about 120 kV. The rise time is controlled by varying the inductances, which couple the output of the VWG to the common point. Typically, this inductance is about 300 μH resulting in a 1 - 2 msec rise time. A 0 - 20 kV dc power supply, capable of an output of about 10 kW is used to charge the high-voltage source capacitor C_1. To generate the high-power rep-rate pulses this capacitor is discharged repetitively through the thyratron V_2 into the pulse transformer, T_2. The output voltage dependence on the dc charge voltage is shown in Figure 2-4.

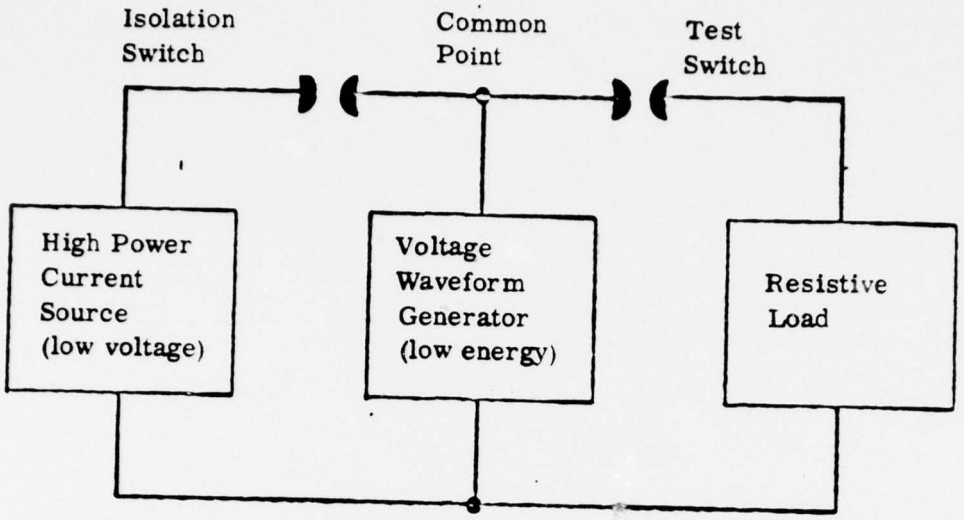

Figure 2-1. Simplified switch test circuit

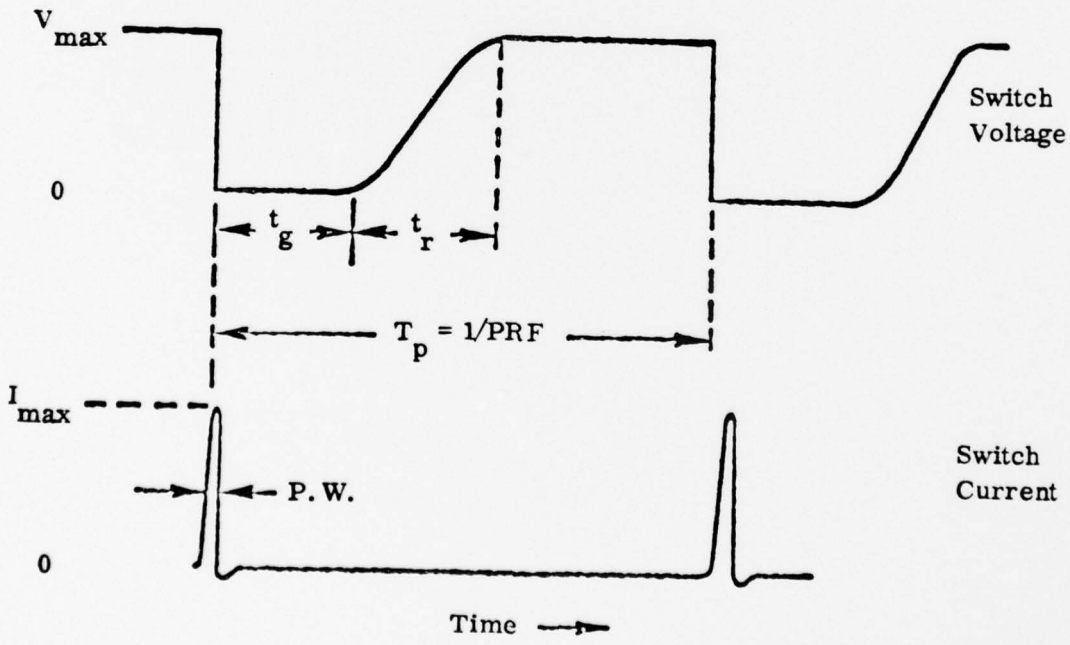

Figure 2-2. Idealized switch voltage and current waveforms. (P.W. - pulse width, t_g - grace period, t_r - rise time, T_p - interpulse period)

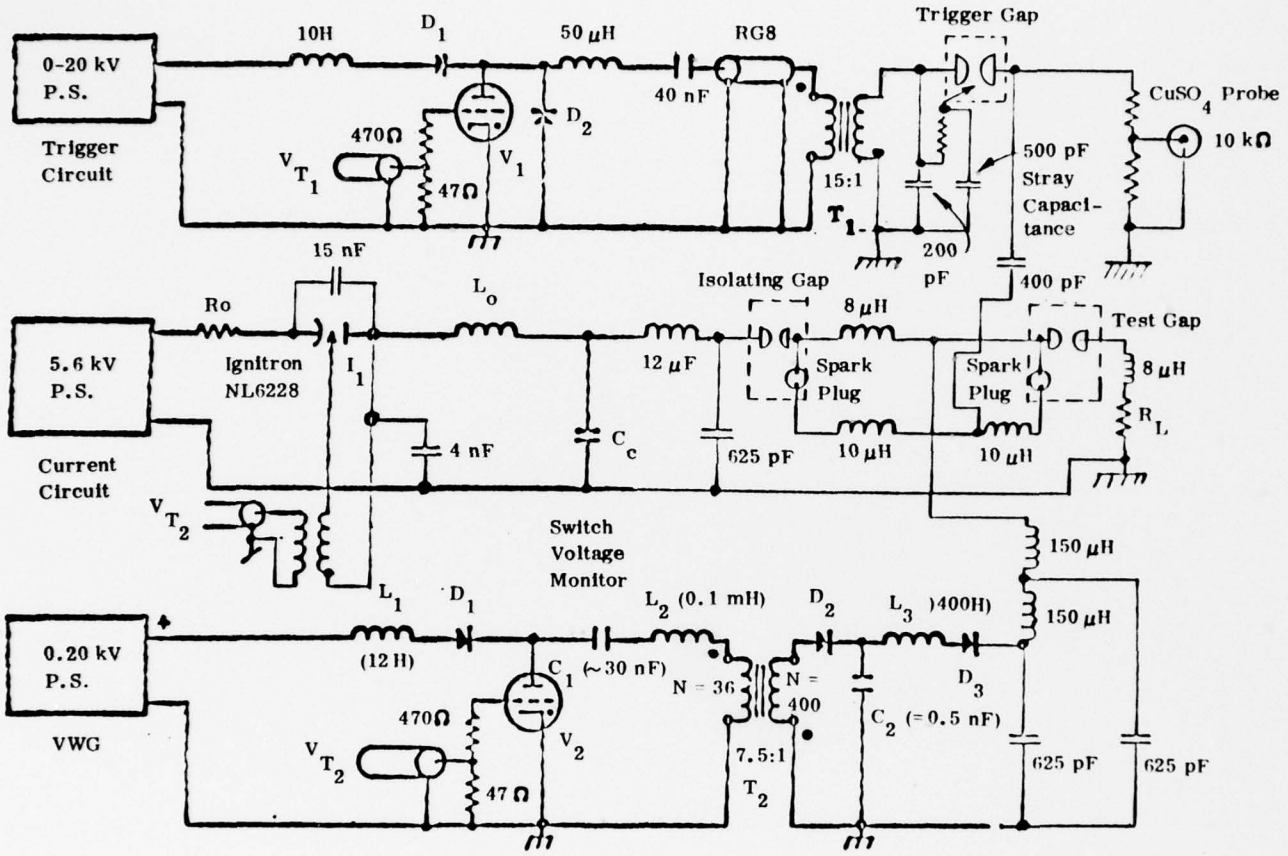

Figure 2-3. Updated circuit diagram for the Maxwell Laboratories, Inc. High Power Switch Test Facility.

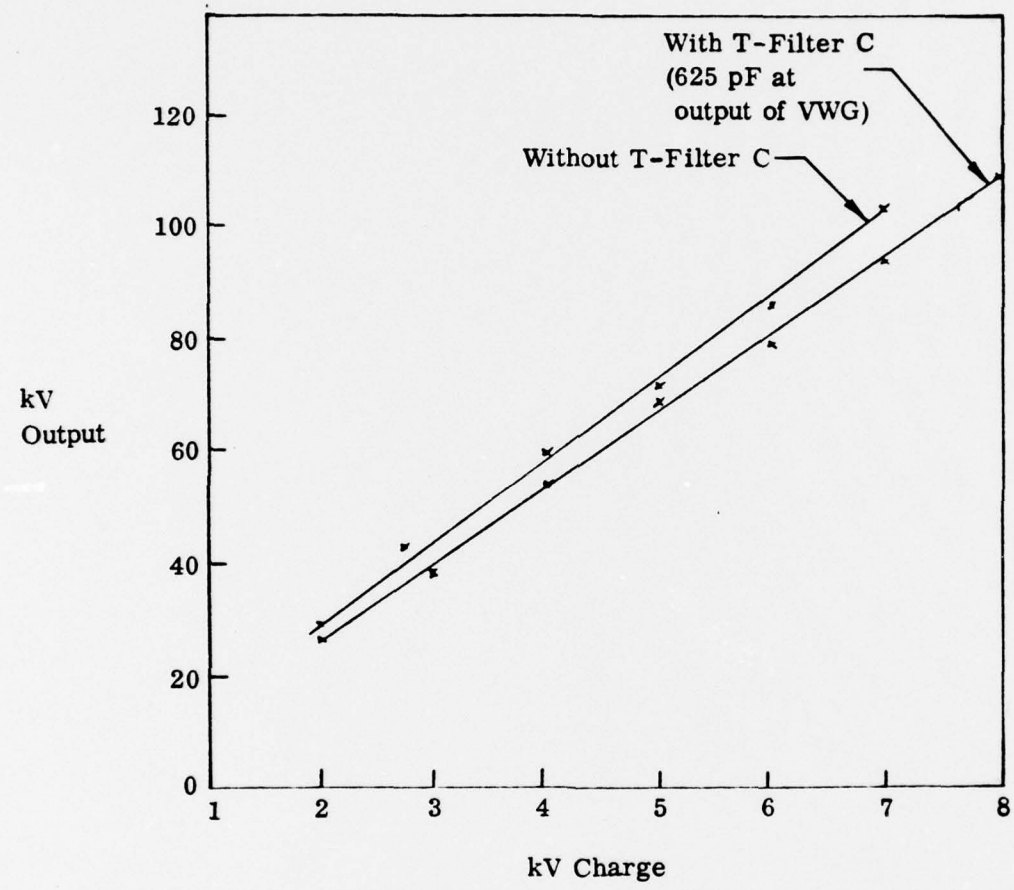

Figure 2-4. Waveform generator output voltage vs charge voltage

2.1.2 Diagnostics

An oil-immersed resistive divider, sketched in Figure 2-5 provides the monitor waveform which is routinely recorded on the magnetic tape recorder. To view the VWG monitor output in real time, the monitor is connected to a memory oscilloscope and the VWG is operated without the current source. The waveforms at 100 pps and 150 pps, are shown in Figure 2-6. The first two pulses are lower than peak because several cycles are required to resonantly charge C_1, through the charging indicator L_1. This can be seen in the figure as two vertical steps prior to reaching peak.

The initial burst of $\approx$50 pulses are higher in amplitude than the remaining pulses. Then, the amplitude exponentiates down to a final value after $\simeq$50 pulses because of the nonzero internal impedance of the 0 - 20 kV power supply; the voltage reduction depends on power output as shown in the comparison of 100 pps and 150 pps. The power supply can be viewed as a charged capacitor. The sequence of output pulses causes this capacitor to discharge until the power delivered to the circuit equals that taken from the power source. This voltage variation could have been effectively avoided by starting the current and trigger sources after $\simeq$50 pulses elapsed.

2.1.3 Calibration

To calibrate the oil-immersed monitor a pair of Tektronix HV probes were connected in parallel with the oil-immersed monitor to monitor the common point. The Tektronix probes are limited to $\simeq$40 kV; therefore a resistive divider is required to expand the probe range to $\simeq$100 kV. The following procedure was used.

1. Two Tektronix 1000-1 (100 MΩ input impedance) probes were connected to the common point. The waveform generator was operated at 50 pps (40 kV). The two probes delivered the same voltage to the oscilloscope indicating their calibrations were the same.
2. One probe was left in the same position; the other was connected to a series string of resistors as shown in Figure 2-7.

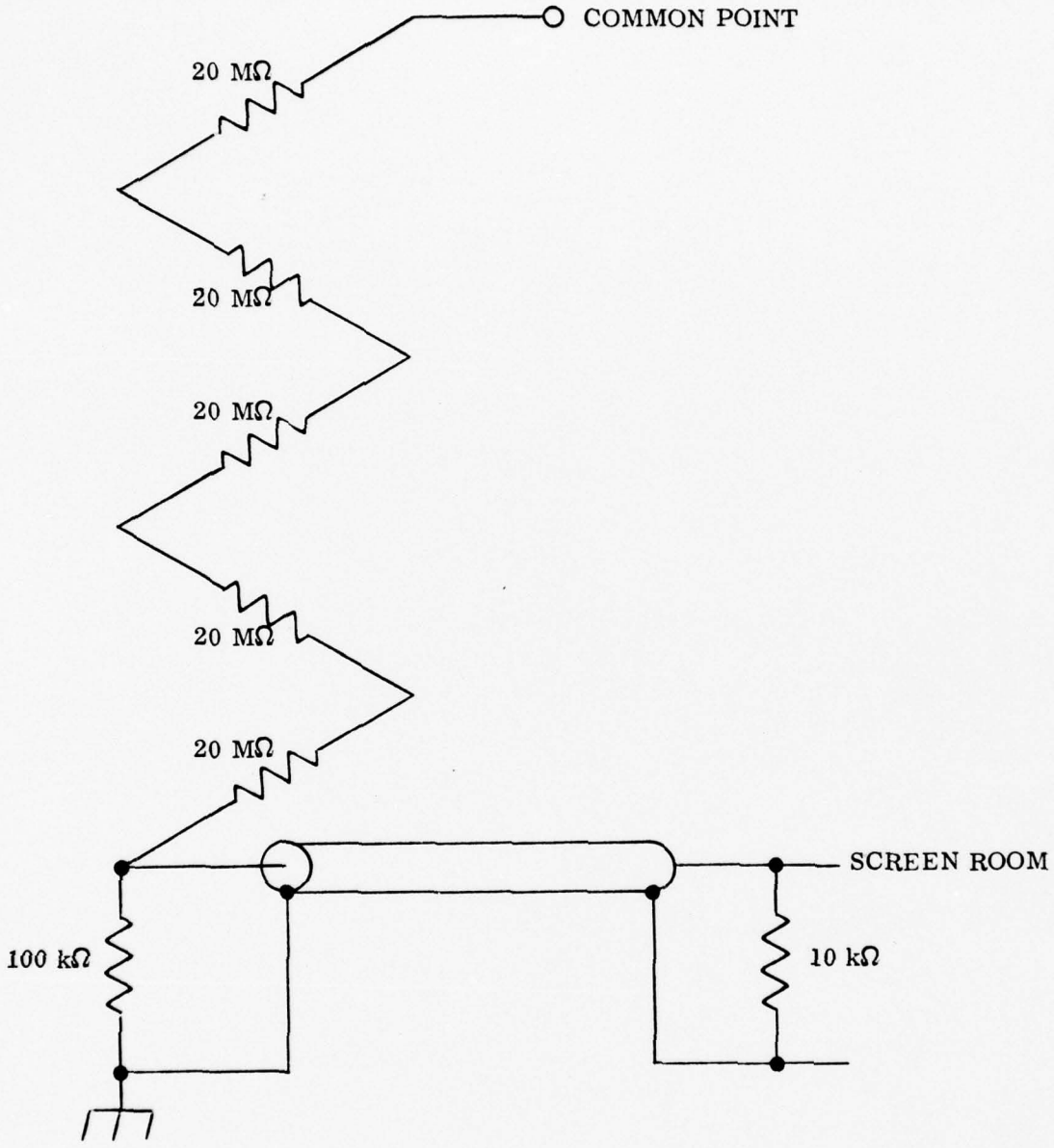

Figure 2-5. Oil-immersed resistive divider

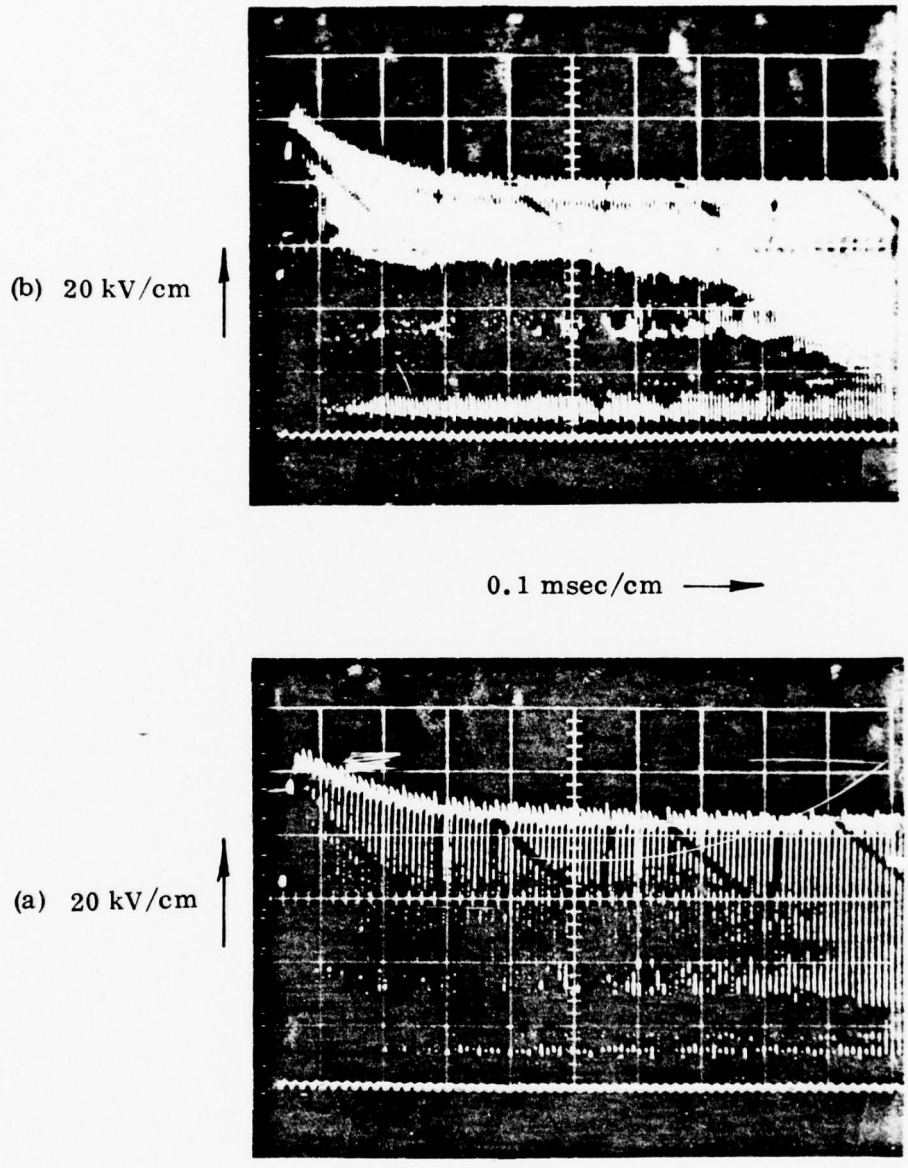

Figure 2-6. VWG waveforms. Power source not connected.
(a) 100 pps
(b) 150 pps
20 kV/cm, 0.1 msec/cm

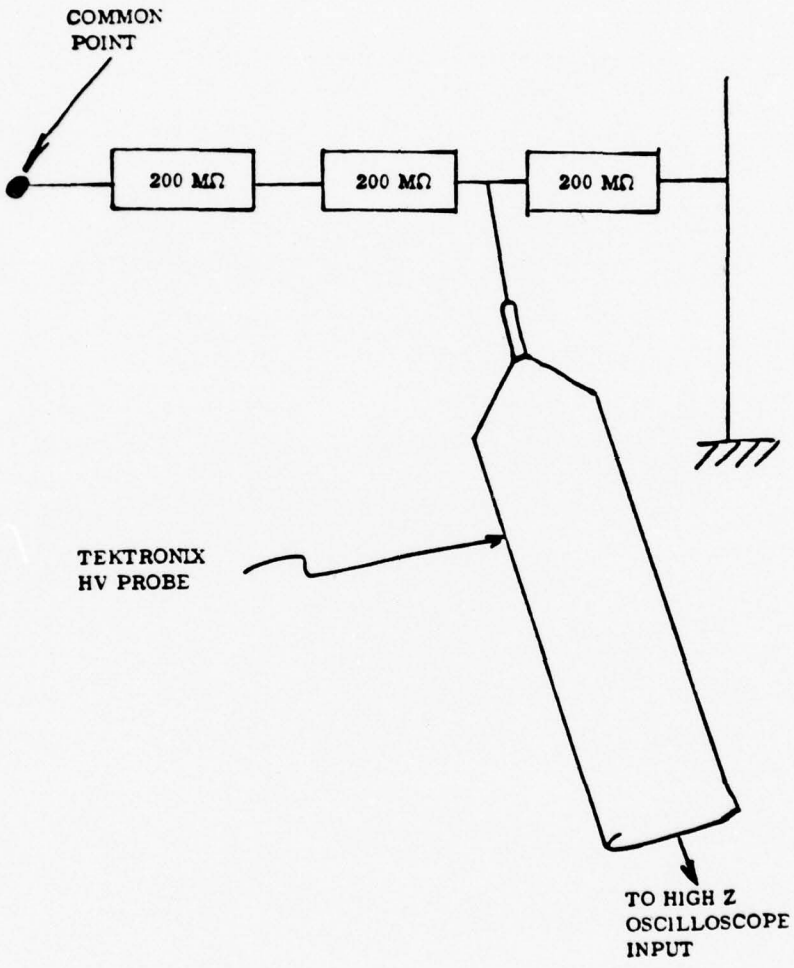

Figure 2-7. Divider used to extend 40 kV Tektronix probe to 100 kV

3. The system was operated at 20 kV. The voltage calibration was 10:1 for the divider formed by the monitor and three resistors. This attenuation was then checked at 40 kV and found to be constant. Typical waveforms are shown in Figure 2-8.

With this equipment, the common point can be driven to $\gtrsim$ 100 kV while applying $\simeq$ 10 kV to the probe.

2.2 CURRENT SOURCE

2.2.1 Description

The main power source is provided by the 1 MW power station constructed by Maxwell for the previous Wright-Patterson switch program. The power station has three transformers which convert 3-phase 12 kV into 4160 V which is brought into the laboratory and rectified as shown in Figure 2-9. The pulsating, full wave dc is then connected to the current-source capacitor C_c which rings-up to the dc charge voltage of 8 kV. C_c is composed of a set of four 14 μF capacitors which can be connected in various parallel arrangements to attain the desired source capacitance.

The current waveform depends on circuit inductance, load resistance and source capacitance. The overall objective of this circuit is to attain a specified peak current and charge transfer to provide simulation of a high-power circuit.

The circuit is setup to be under damped to the extent that 20 - 25% reversal occurs thereby enabling the ignitron to commutate. A typical circuit inductance is 25 μH which enables a current waveform of about 50 μsec FWHM to be obtained with peak current in the range of 3 to 6 k amp.

Circuit inductance is provided by lumped constant inductors fabricated from wire formed into spiral windings. The switch and distributed inductance comprise less than 1/2 μH (Fig. 2-3). About 8 μH is placed between the test switch and the load and 12 μH is placed between the isolation switch and the source. These inductors prevent too-rapid a collapse in trigger voltage in the event one of the switches triggers early. Another advantage accrues from the inductor which is placed near the source; the 12 μH helps alleviate ignitron prefiring problems by isolating it from the trigger pulse. The remaining circuit inductance is between the switches.

(a) Tektronix Probe (1000:1)
Connects to resistive divider
$\hat{v}$ = 3.5 cm x 13.6 kV/cm
= 48 kV
rep rate = 20 pps
(13.6 kV/cm results
from calibration)

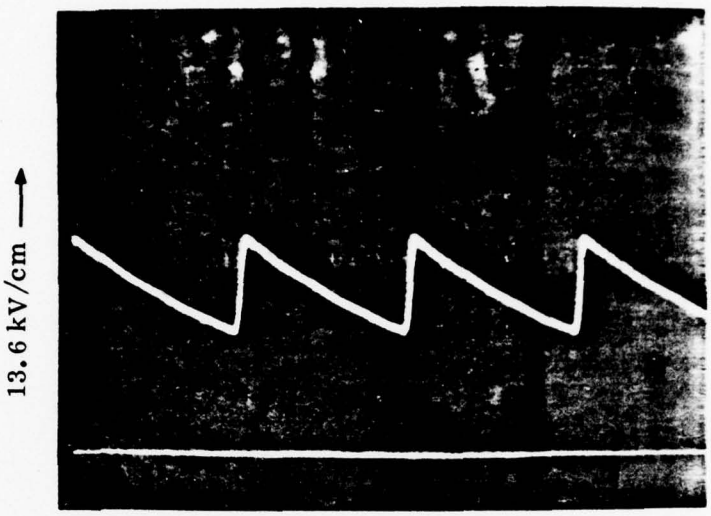

Tektronix Probe Direct Connection
to common-point

$\hat{v}$ = 5.0 cm x 10 kV/cm
= 50 kV

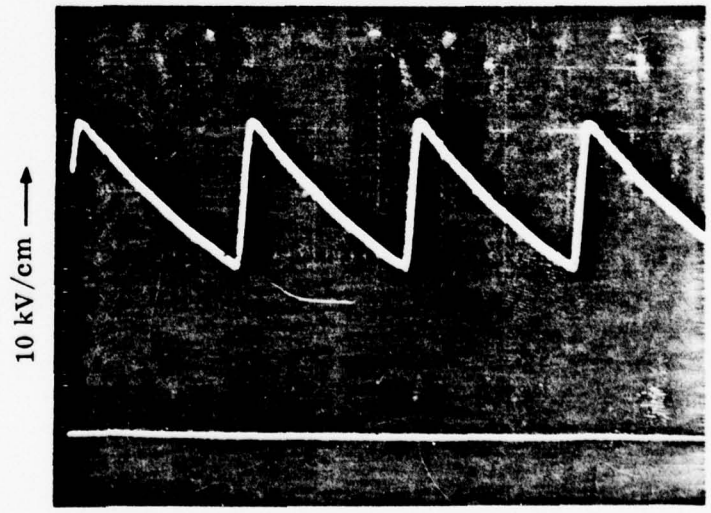

Figure 2-8. Voltage waveform generator output waveforms from Tektronix HV probe

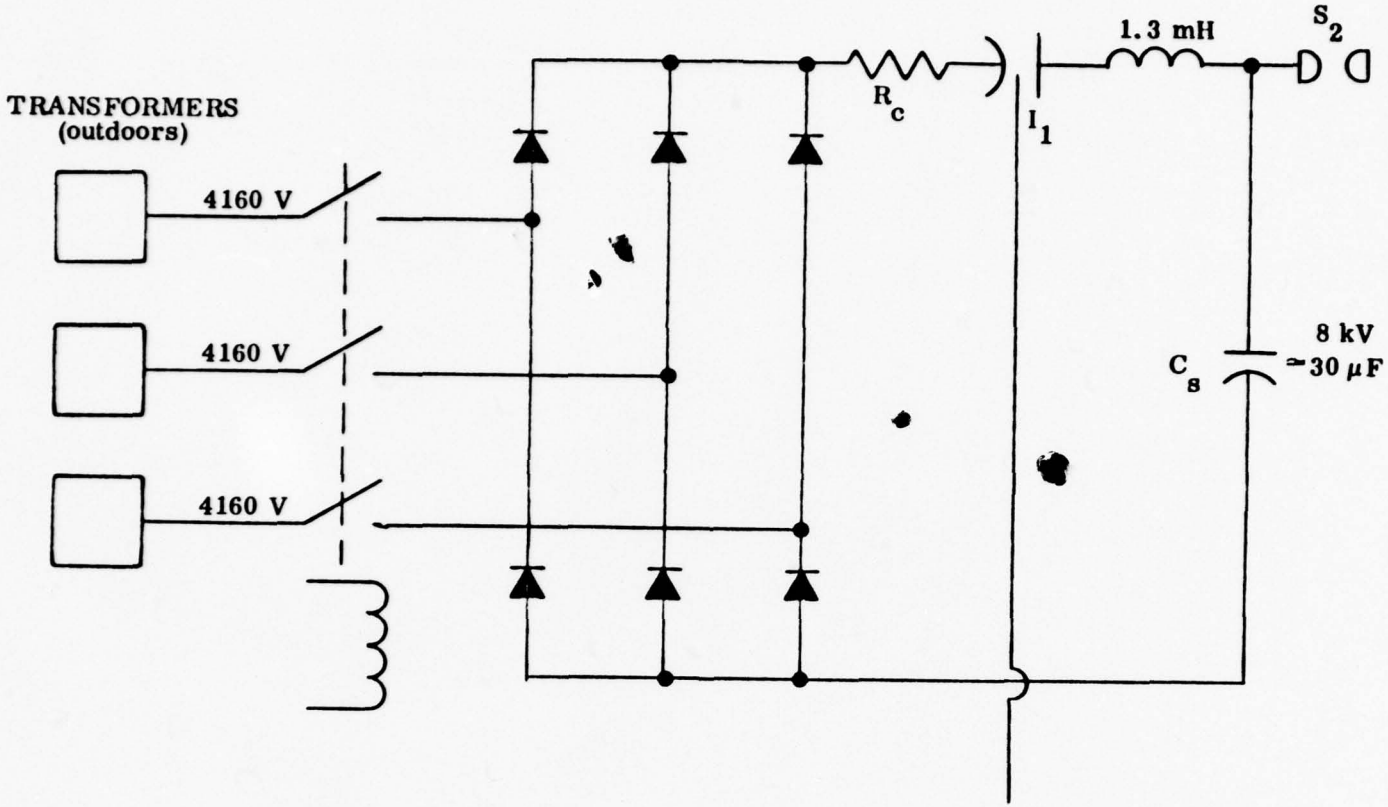

Figure 2-9. Main power source. 4160 volts, 3-phase with 1 MW capability is rectified to provide pulsating dc, rms = 5.6 kV dc which resonantly charges C_s to 8 kV

2.2.2 Diagnostics and Calibration

A Pearson current probe measures the current through L_c to determine the recharge current to C_c when the switches are open-circuited. This waveform is relatively slow ($\approx$1 msec duration) and is routinely displayed on a magnetic tape recorder.* The main use of this waveform is to show C_c (see Fig. 2-3) consistently recharges after a trigger pulse has fired the ignitron I. Lack of recharge current occurs if the isolation or test gap does not break down.

The discharge current through R_L is also measured with a Pearson probe. This waveform is not routinely measured during a rep-rate shot sequence. The waveform is obtained during system calibration, especially when a circuit parameter has been changed. Figures 2-10 and 2-11 show overlays of several hundred load waveforms corresponding to the charge voltage of 60 kV.

2.3 TRIGGER GENERATOR

2.3.1 Description

The trigger generator, provides a fast rise time waveform of about 150 kV to the common point between the test and isolation switches. A trigger gap insulates the 400 pF coupling capacitor from the output of the trigger generator transformer. This 400 pF capacitor, connected between the common point and the trigger generator output, is charged by the VWG prior to launching the trigger pulse.

When the trigger gap breaks down, the trigger voltage is added to the VWG voltage on the common point. This assures adequate voltage to breakdown the test and isolation gaps nearly simultaneously. As shown in Figure 2-3, the 400 nF capacitor is charged by current passed through the spark plugs which irradiate the negative electrodes and reduce jitter in the switches. Power requirement for the trigger generator is about 1 kW at 250 pps.

*The magnetic tape recording system is described in ref. 1, Section 2.2.

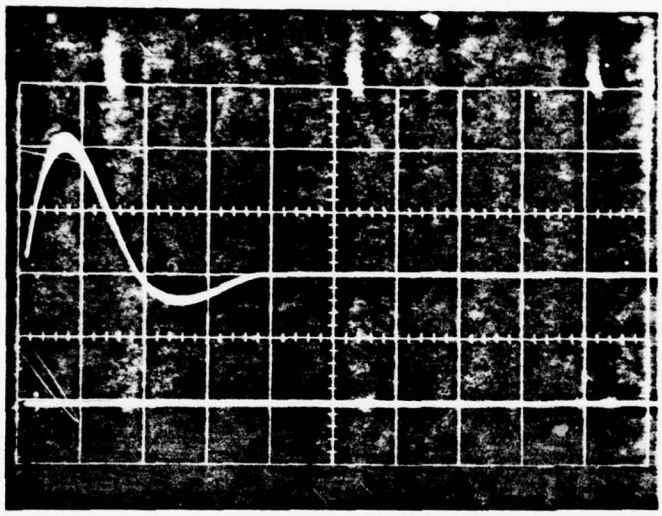

50 μsec/ cm ⟶

Probe sensitivity:

$$y = \frac{10\ \text{V/cm}^{(\text{scope})}}{0.005\ \text{V/amp}} = 2\ \frac{\text{k amp}}{\text{cm}}$$

$$\hat{I} = 2.2\ \text{cm} \times 2\ \frac{\text{k amp}}{\text{cm}} = 4.4\ \text{kA}$$

reversal = 22%

Figure 2-10. Load Current Into $R_L = 0.88\Omega$, $C_c = 8$ kV, $V_o = 60$ kV. Sensor is a Pearson probe mod. 301A which has 0.01 V/amp sensitivity unterminated and 0.005 V/amp when terminated in 50Ω as in the present case. prf = 250 pps.

$$y = 5 \text{ V/cm} \times \frac{1}{0.005 \text{ V/amp}}$$

$$= 1 \frac{\text{kamp}}{\text{cm}}$$

$$\hat{I} = 3.4 \text{ kamp}$$

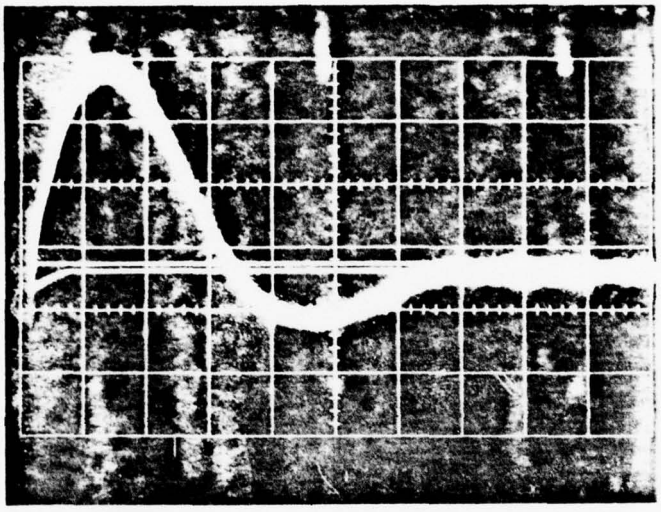

$$20 \frac{\mu\text{sec}}{\text{cm}}$$

Figure 2-11. Overlay of ~100 Load Current Waveforms. V_o = 8 kV, V_o = 60 kV, R_L = 1.8Ω, C_c = 120 mC 200 pps. Run date, 2/15/77.

2.3.2 Diagnostics and Calibration

A $CuSO_4$ resistive divider monitors the output of the trigger generator. Figure 2-12 shows output trigger voltage (without VWG operating) (a) with, and (b) without the switches in position. The oscillation observed in the latter waveform are caused by the resonance setup between the trigger generator and the main switch discharge circuit. This resonance occurs when the isolation and output switches close thereby connecting the high impedance trigger generator to the relatively low-impedance current circuit. This oscillation has no impact on switch performance (coulomb or peak current rating) because the oscillations persist for only about 1 μsec, and the trigger circuit impedance is hundreds of Ohms compared to the main discharge circuit which is less than one Ohm.

2.4 PNEUMATICS

2.4.1 Description

The air system provides rapidly moving air to purge the switches between closures. Compressed air at $\simeq$ 100 psig is initially stored in a 60 ft^3 cylindrical tank about 19 ft in length and 3 ft in diameter. Identical tubing and valve assemblies convey the compressed air through the two switches. A regulator in each tube reduces the pressure to about 35 psig, the pressures at which the switches operate. Tubing length is about 30 ft extending from the pressure tank to the switches. A detailed diagram is shown in Figure 2-13.

The air flow in Configuration I switches differs from that in Configuration II. In Configuration I symmetrical air inputs around the outer circumference of each of the electrode end plates are provided the air exits through the hollow electrodes. A 3-inch ID tube probides flow for each of the two switches.

In Configuration II, each switch has two inputs; one radial and one axial through one of the hollow electrodes. The exhaust is taken from the other hollow electrode opposite the input port. Figure 2-14 shows a flow

(a)

y = 106 kV/cm

v_c = 12.5 kV charging

y = 170 kV into 10 kΩ Probe

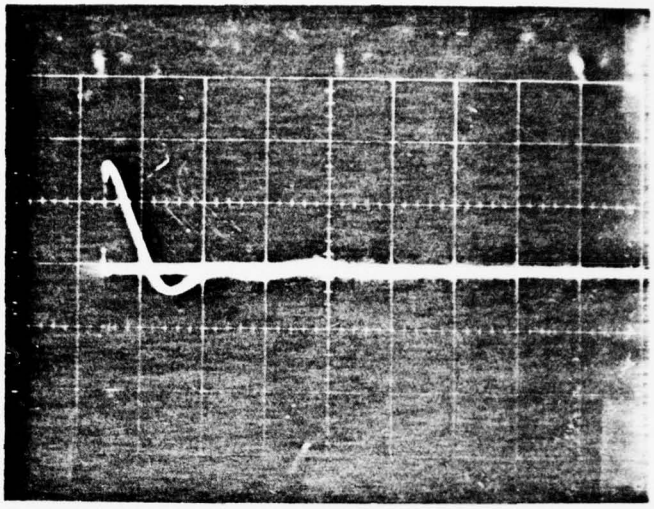

x = 5 μs/cm ⟶

(b)

Trigger Output With
Switches Connected

$P_{main\ gap}$ = 34 psig (static)

$P_{trig.\ gap}$ = 42 psig (static)

V_{chg} = 10 kV

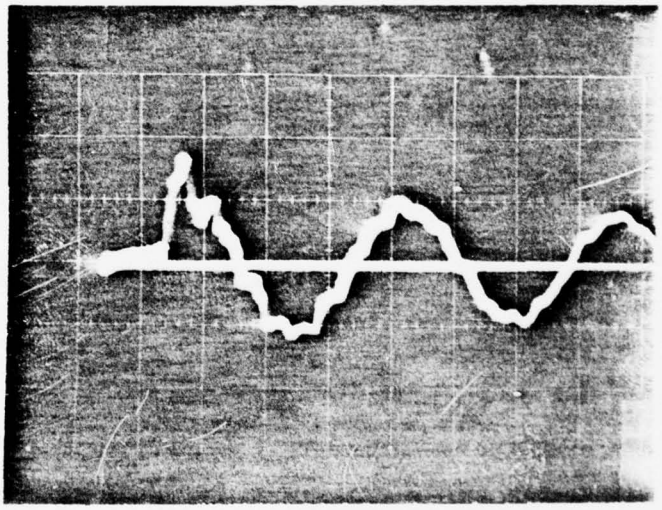

53 kV/cm ⟶

100 ns/cm ⟶

Figure 2-12. Trigger generator output (a) without switches and (b) with switches in position

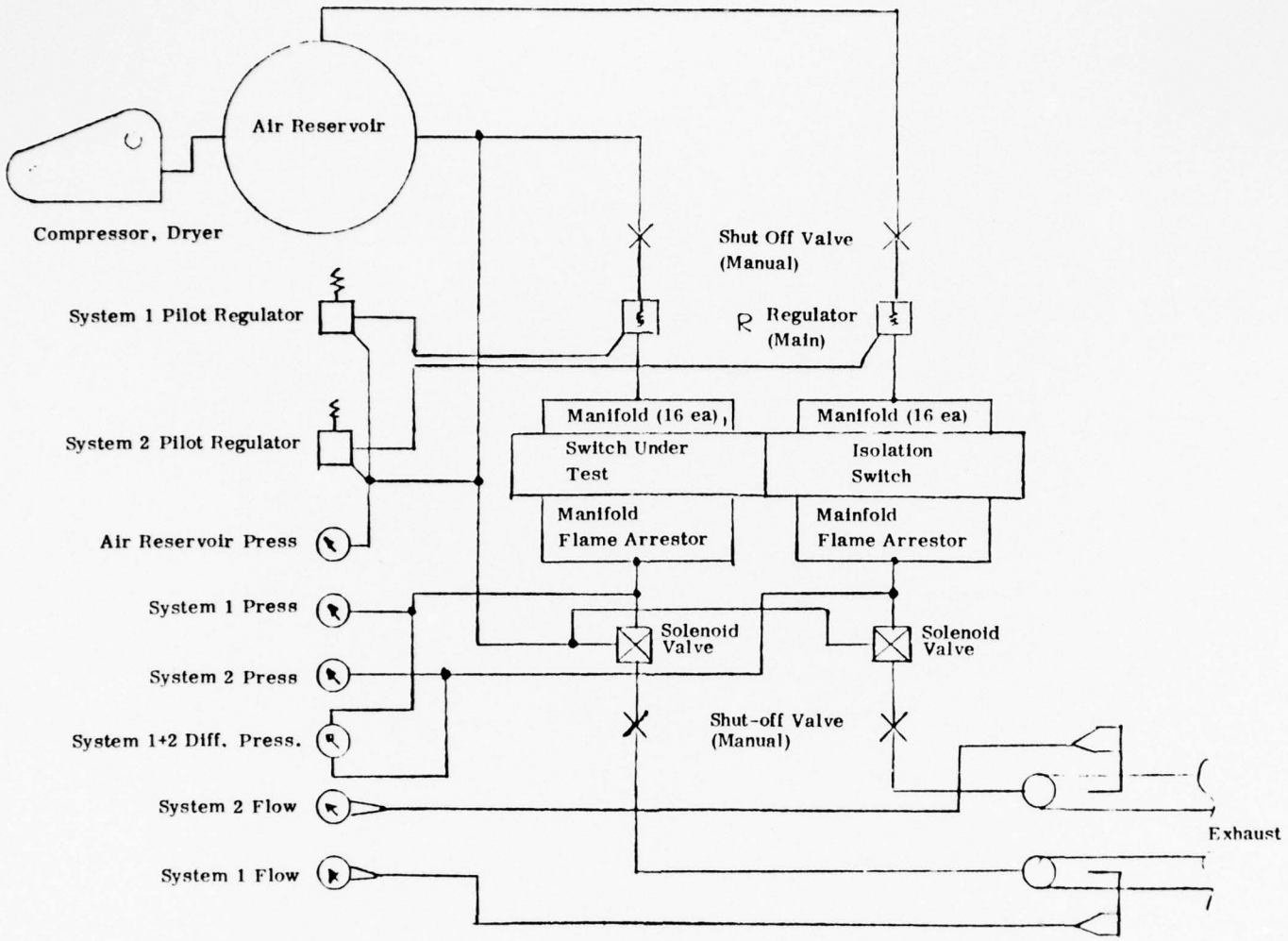

Figure 2-13. Air system schematic diagram for Configuration I switches (single input port per switch)

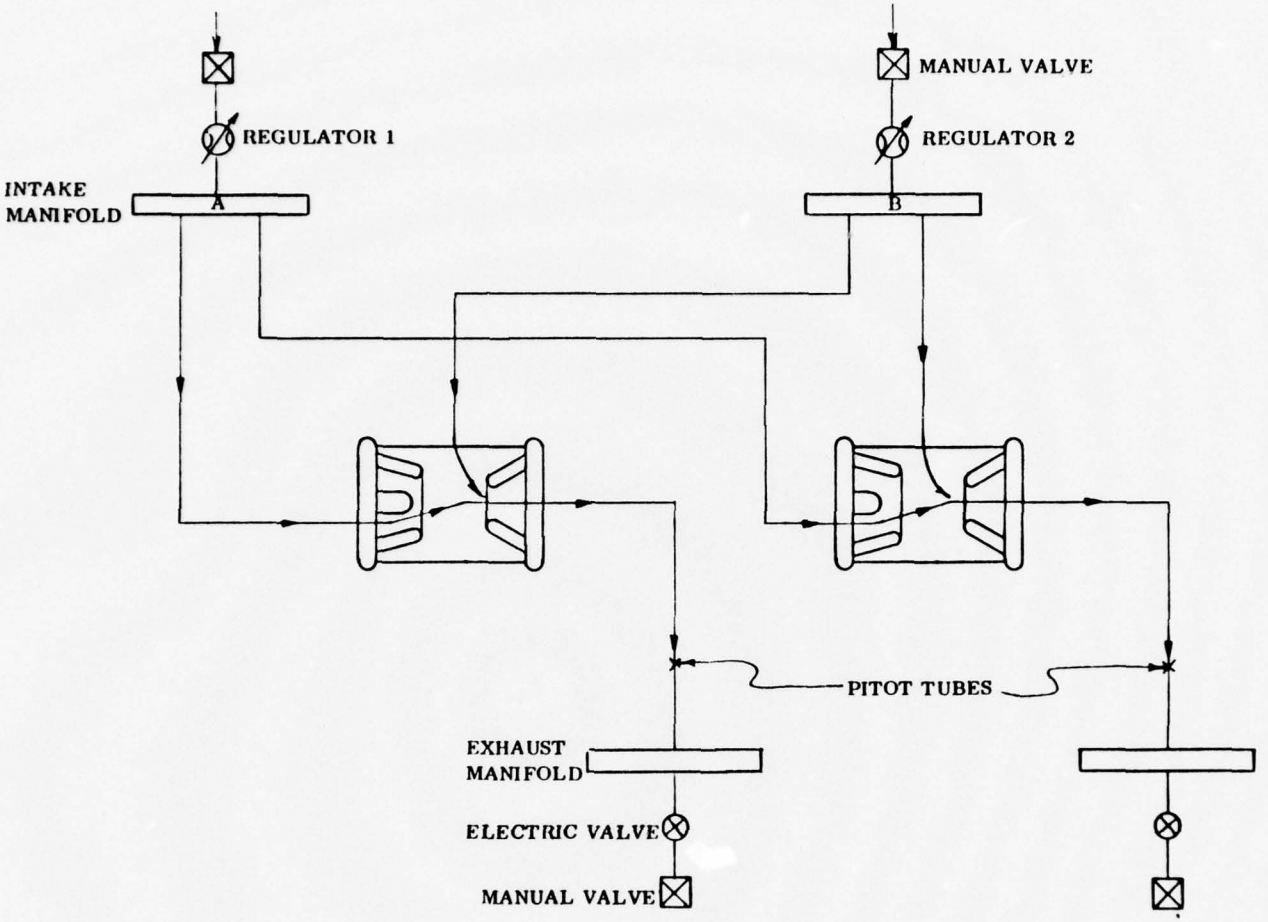

Figure 2-14. Air-flow diagram for Configuration II switch test

diagram for the Configuration II case. One of the 3-inch ID tubes from the reservoir connects to the radial inputs of both switches. The other 3-inch ID tube connects to the axial inputs to both switches. Therefore, independent control of radial and axial flow is maintained and both switches have identical flow rate.

2.4.2 Diagnostics and Calibration

A pressure gauge measures static pressure at the gas-input end of each switch. A pitot tube measures exhaust velocity in the output tubing of the switches.

A separate static pressure measurement is obtained from the air reservoir.

In a typical gas-flow calibration for Configuration II switches, the reservoir was pressurized to 100 psig. Air was allowed to flow for sixty seconds after which the reservoir pressure was 65 psig. Using the ideal gas equation, the total flow rate of 123 SCFM was calculated as shown in Appendix III. This flow passed through two switches, providing 62 SCFM per switch. This compared favorably with the pitot tube measurement of 63 SCFM per switch.

SECTION 3
CIRCUIT OPERATION

This section discusses circuit operation, including the timing of the simulator components.

Consider the start of a cycle as occurring immediately after the isolation and test switches have discharged the current-source capacitor. Figure 3-1 shows circuit timing where t = 0 corresponds to the closure of the switches. At this time, the VWG capacitor C_1, is already recharged and the 40 nF trigger capacitor at the input to the trigger transformer is in the process of recharging, (which requires about 5 μsec; 40 nF through 60 μH).

A preset grace period (1 msec was used during this program) elapses during which the circuit is quiescent; flowing air continuously purges the gaps in preparation for the next recharge from the VWG.

After the grace period a trigger pulse fires the ignitron I_1, to recharge the current-source capacitor C_c, and simultaneously another trigger pulse fires the VWG thyratron to apply voltage across the gaps. The VWG waveform has a rise time of $\approx$1 msec. After the VWG erects to peak voltage, the diodes maintain voltage at the common point allowing the VWG thyratron to extinguish. C_1 begins to recharge (in $\approx$ msecs). About 1 msec after the peak voltage is reached (a total of about 4 msec from the previous switch closure for 250 pps rep rate, the trigger voltage is reapplied to break down the gaps, discharge C_c and begin a new cycle. The objective behind delaying the recharge of C_c until the VWG is triggered is to prevent reapplication of voltage across the isolation switch before adequate purge has occurred.

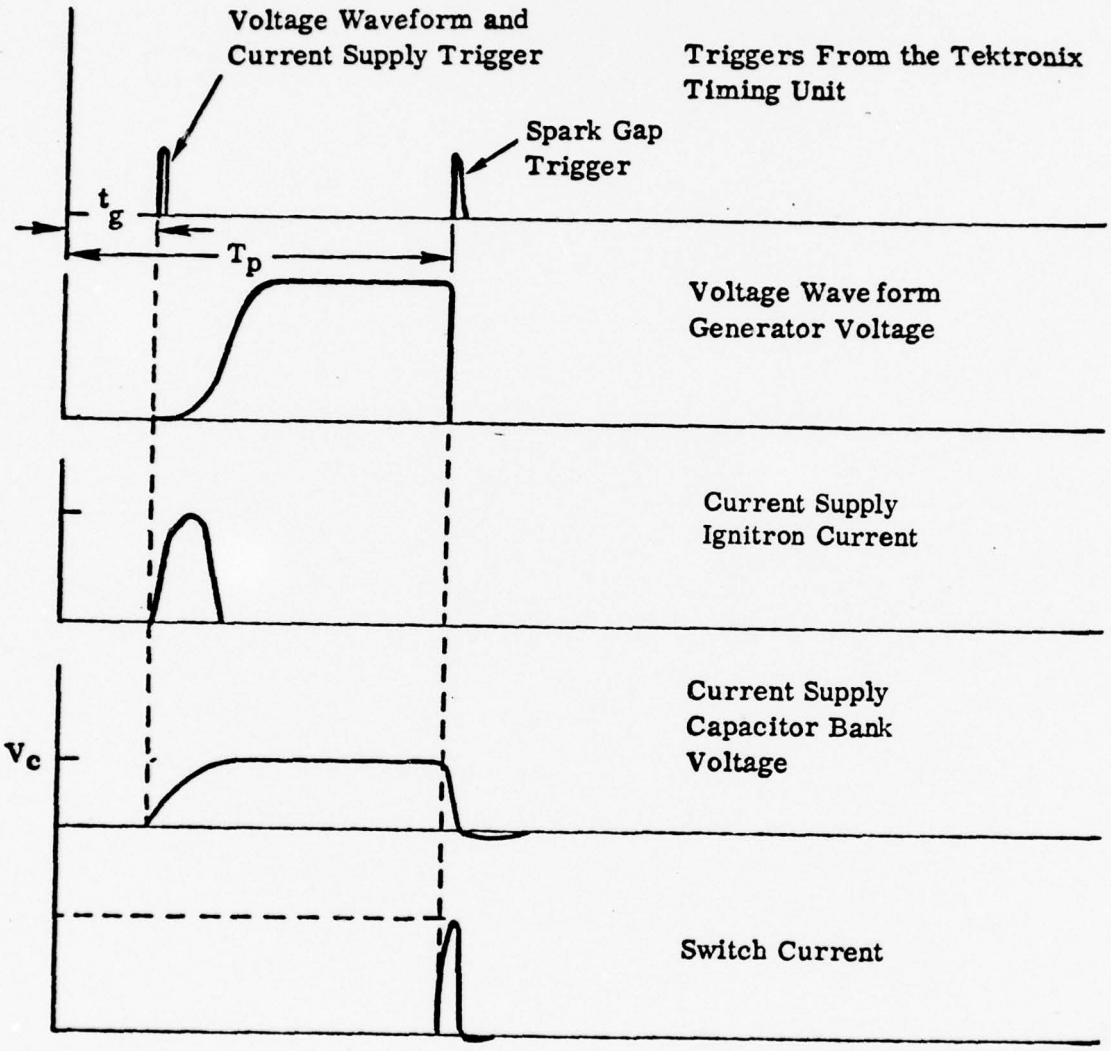

Figure 3-1. Time Sequence of Voltages and Currents in the Switch Test Facility.

A summary of experimental parameters used in Table 3-1 shows the test sequence used for each switch design. Each row contains the operating parameters in a given switch experiment. The objective in this table was to define a sequence of operating levels so that different switch designs could be evaluated depending on the level they achieved.

SUMMARY OF EXPERIMENTAL PARAMETERS

C_c, μF	Current-source capacitor
Q	Charge stored in C_c. Q = CV where V = 8 kV
L_c	Recharging inductor for C_c
R_c	Current limiting resistor in high current circuit
PRF	Pulse repetition frequency (pulse per second)
VWG	Peak output voltage from voltage waveform generator
R_L	Load resistance in current circuit
P_s	Simulated power = PRF x Q x VWG
I_{Load}	Peak load current in test circuit (measured with Pearson probe)
Δt_c	Recharging time of C_c through L_c

TABLE 3-1

TEST SEQUENCE FOR REP-RATE SWITCH
(Each Row Corresponds to a Set of Operating Parameters)

Single Electrode Pair Test Program

Data Ref.:	C_c μF	Q mC	L_c mH	R_c Ω	PRF PPS	VWG kV	R_L Ω	P_S MW	I_{Load} kA
1	7.5	60	9.8	36	100	20	3.5	0.120	1.25
2						40		0.240	
3						60		0.360	
4					150			0.540	
5					200			0.720	
6					250			0.900	
7	15	120	3.2	14.6	100	60	1.8	0.72	3.5
8					150			1.08	
9					200			1.44	
10					250			1.80	
11	30	240	1.4	6.83	100	60	0.88	1.44	4.4
12					150			2.16	
13					200			2.88	
14					250			3.60	
15	45	360	1.4	5.57	100	60	0.59	2.16	6.0
16					150			3.24	
17					200			4.32	
18					250			5.40	
Constants: VWG T_R = 1 msec; T_g = 1 msec; V_s = 8 kV; Air flow: 150 SCFM - Conf. I, 63 SCFM - Conf. II									
11*	30	240	1.4	6.83	100	90	0.88	2.2	4.4
12*					150			3.2	
13*					200			4.3	
14*					250			5.4	
T_R = 2 msec; T_g = 1 msec; V_s = 8 kV; Air flow: 63 SCFM - Conf. II									

*Maximum power tests

SECTION 4

EXPERIMENTAL RESULTS

4.1 CONFIGURATION I TEST

The Configuration I switch, shown schematically in Figure 4-1, was tested successfully to the performance level of row 14, Table 3-1. When the next level (360 mC) was attempted to attain row 15, the switch prefire frequency became excessive as shown in Figure 4-2. When prefires occur the common-point voltage (c) is observed to have an irregularity during the rising portion because the switch prefire discharges the common point to zero voltage. The response of the recording system is too slow to show the return to zero because immediately after the prefire the common point begins to be recharged by the VWG. However, the VWG source capacitor C_1 is already partially discharged before the prefire. Therefore, the VWG cannot reach full voltage after a prefire, as shown by the reduced amplitudes in (c).

The double-pulse associated with the trigger generator (d) creates the suspicion the trigger generator was causing the prefires. Other evidence indicates the trigger was not prefiring; rather the electronic pulse generator in the diagnostic room which creates the pulse observed on the record was triggering from the VWG waveform. For example, the prefire in the middle of the record occurred at so low a voltage, the trigger-pulse generator failed to show the double pulse, confirming the fact the VWG is triggering the diagnostic pulser, rather than vice versa. (That monitoring technique was thereafter modified to trigger from the low-level trigger generator rather than the VWG.)

Specifications of the Configuration I switch test are the following:

Gap length	0.5 cm
Flow rate	145 SCFM
Max charge transfer successfully attained	240 mC

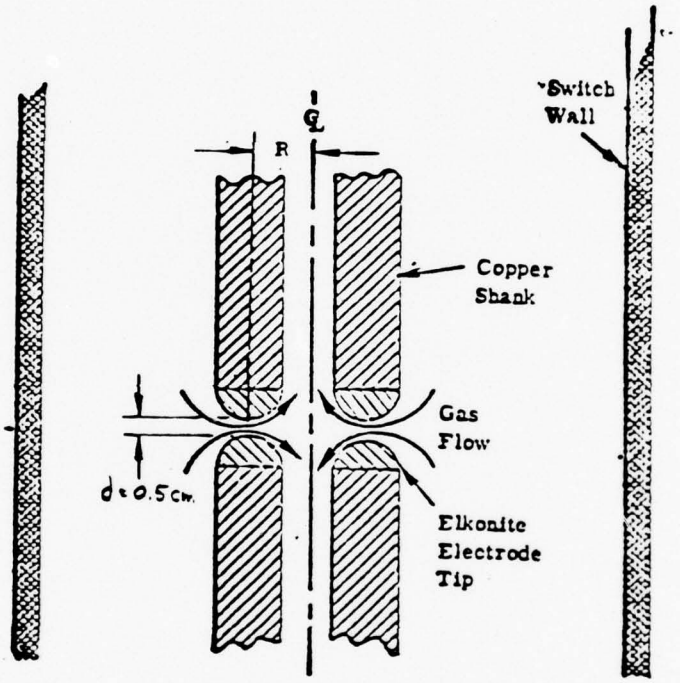

Figure 4-1. Schematic of Configuration I switch

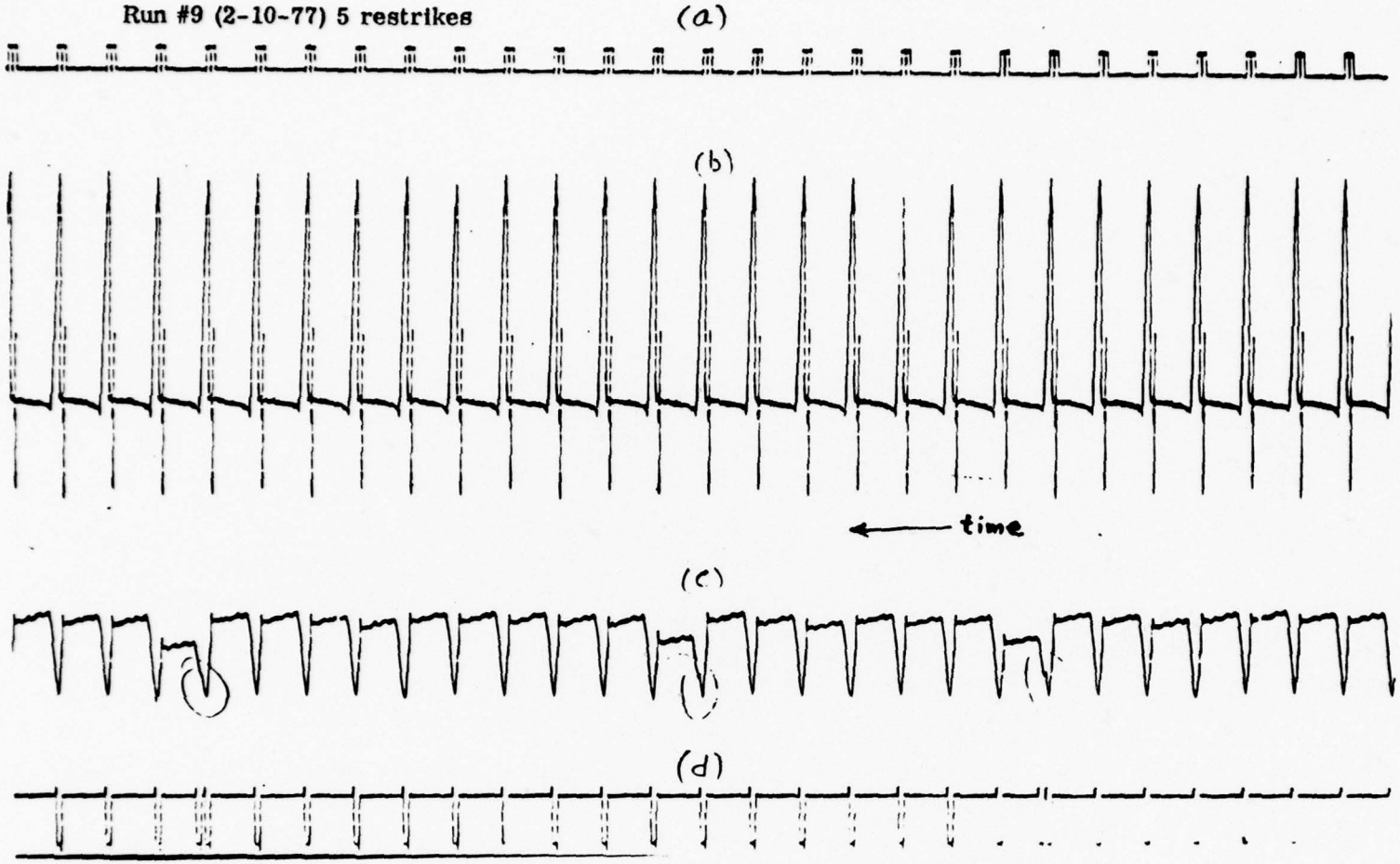

Figure 4-2. Run #9 (250 pps) of Configuration I switch, showing prefires (circled). Magnetic tape record of (a) ignitron trigger, (b) recharging current waveform, (c) voltage waveform generator output (common point), (d) trigger to trigger generator (see text)

Performance level successfully attained	Row 14, Table 1
Maximum voltage	60 kV
Rep rate	250 pps

4.2 CONFIGURATION II TEST (d = 1.5 cm)

The Configuration II switch is shown in Figure 4-3. The maximum level of the Configuration II (d = 1.5 cm) switch was 3.6 MW, associated with Row 14, Table 3-1. Figure 4-4 is a typical magnetic tape record which shows the beginning of the burst. The first few irregularities in the recharge current are caused by insufficient VWG voltage which normally occurs at the start of the burst until the resonance charging system develops full voltage. Once full VWG (60 kV) voltage is attained, the switch operated with virtually no prefires or no-fires on that run. The reduction in VWG amplitude which is observed as time progresses from right to left was discussed in the section on diagnostics. Configuration II switch parameters in this test were:

Gap length: 1.5 cm

Air flow: 40 SCFM

$Q = 240$ mC

$V = 60$ kV

$P = 3.6$ MW

Performance was not consistant from run-to-run. Sometimes, prefires occurred early in the charging waveform, causing lock-ons which damaged the switch envelope. To reduce prefire probability and attain higher power, switch gap spacing was increased to 2.0 cm.

4.3 CONFIGURATION II TEST (d = 2.0 cm)

Configuration II tests conducted with 2.0 cm gap spacing enabled Row 14 to be attained, at 90 kV rather than at 60 kV. These parameters are indicated with an asterisk in Table 3-1. This resulted in the power of 5.4 MW. Figure 4-5 shows a typical recharge waveform obtained at maximum power, 5.4 MW at 90 kV. The absence of a recharge waveform at the left-hand

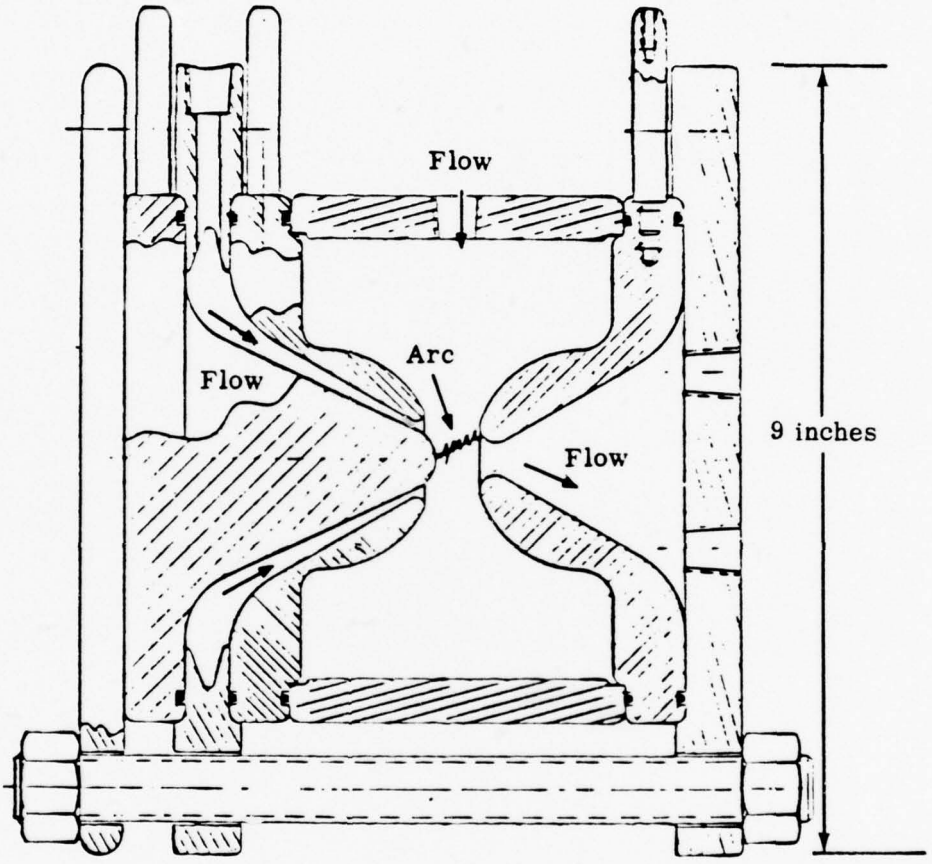

Figure 4-3. Configuration II rep rate spark gap switch assembly, SK 68146

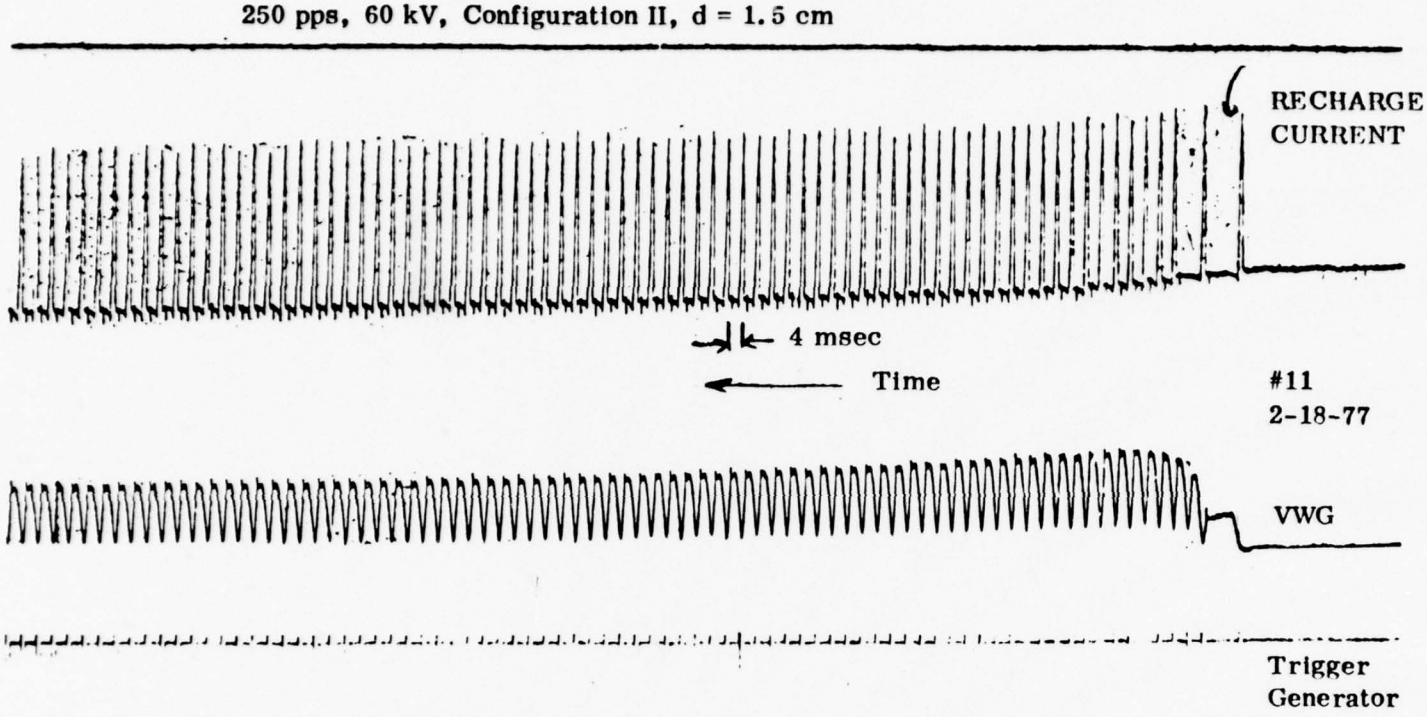

Figure 4-4. Magnetic tape record of recharge current and common-point voltage waveform for Configuration II switch with d = 1.5 cm

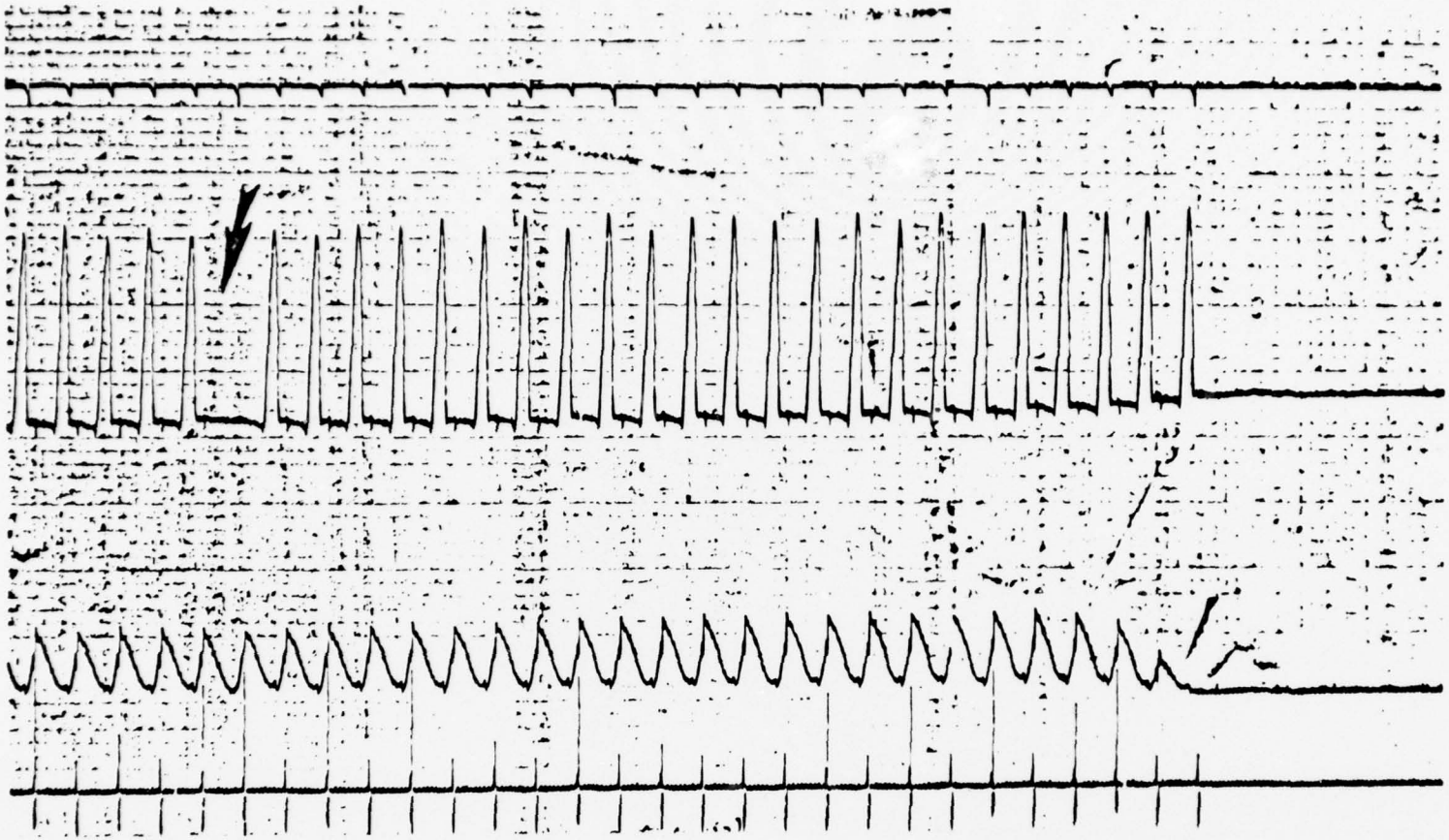

Figure 4-5. 250 pps Sequence (Run #9 5-6-77) Showing a no-fire of the isolation switch.

side of the trace indicates a no-fire of the isolation switch. In the total 11 second run of about 3000 pulses, 11 such no-fires occurred. In no case did a pre-fire occur. The latter observation is important because in future work, increasing trigger amplitude and rise time could further reduce no-fire probability presumably to nearly zero. In two cases (on run #9) neither switch fired. An example of this is shown in Figure 4-6 where the voltage is seen to rise in two steps; the second occurred because the switches did not remove the voltage from the previous charge.

Based on this experiment, the probability of no-fires appears to be $\approx 10^{-3}$. However, the probability of prefire cannot accurately be assessed because none occurred in the last series of runs. For the present, all that can be said is no-fire probability is $< 10^{-3}$. Table 4-1 summarizes maximum power data. For comparison of waveforms, a normal run of 150 pps is shown in Figure 4-7.

A major problem in attaining voltage in the 100 kV range was the elimination of spurious trigger signals. Prefires and lock-ons to be described, were caused by occasionally false-triggering of the SCR trigger generator which fires the ignitron of the main power source. Elimination of these problems required double-shielding, especially of the trigger components.

The upper limits of the 2 cm, Configuration II gap is not clearly defined at this time. The experimental difficulties which attended the rise in voltage and operating power were more related to the shielding of the trigger apparatus than to problems inherent in the switches. It is evident the switches can operate at $\approx$105 kV - 110 kV, because early in each run they did, in fact, operate at that level corresponding to the peak power of 6.3 MW for that brief period of time.

Lack of precision in triggering of either the power ignitron or the trigger generator sometimes causes the switches to enter a conducting phase in which several k amp flows through the switches directly from the power supply. In that case, the ignitron does not extinguish. Current may

TABLE 4-1

OPERATING PARAMETERS AT MAXIMUM POWER

I = 4.5 kA

Q = 240 mC (30 μF and 8 kV chg)

V = 90 kV from VWG

- First VWG pulses are 105 - 110 kV. Then amplitudes exponentiate down to 90 kV.
- When VWG was run at 110 - 120 kV at start in order to settle down to 100 kV, circuit problems (not switch problems) occurred.
- FWHM = 50 μsec.
- Latest run burst $\simeq$ 11 sec at P_s = 5.4 MW.
- At start P_s = 240 mC x 250 x 105 kV
  = 6.3 MW.
- No fire probability $\approx 10^{-3}$ τ_{grace} = 1 msec
- Prefire probability $< 10^{-3}$ τ_{rise} = 2 msec
- Flow rate $\approx$ 60 SCFM per switch

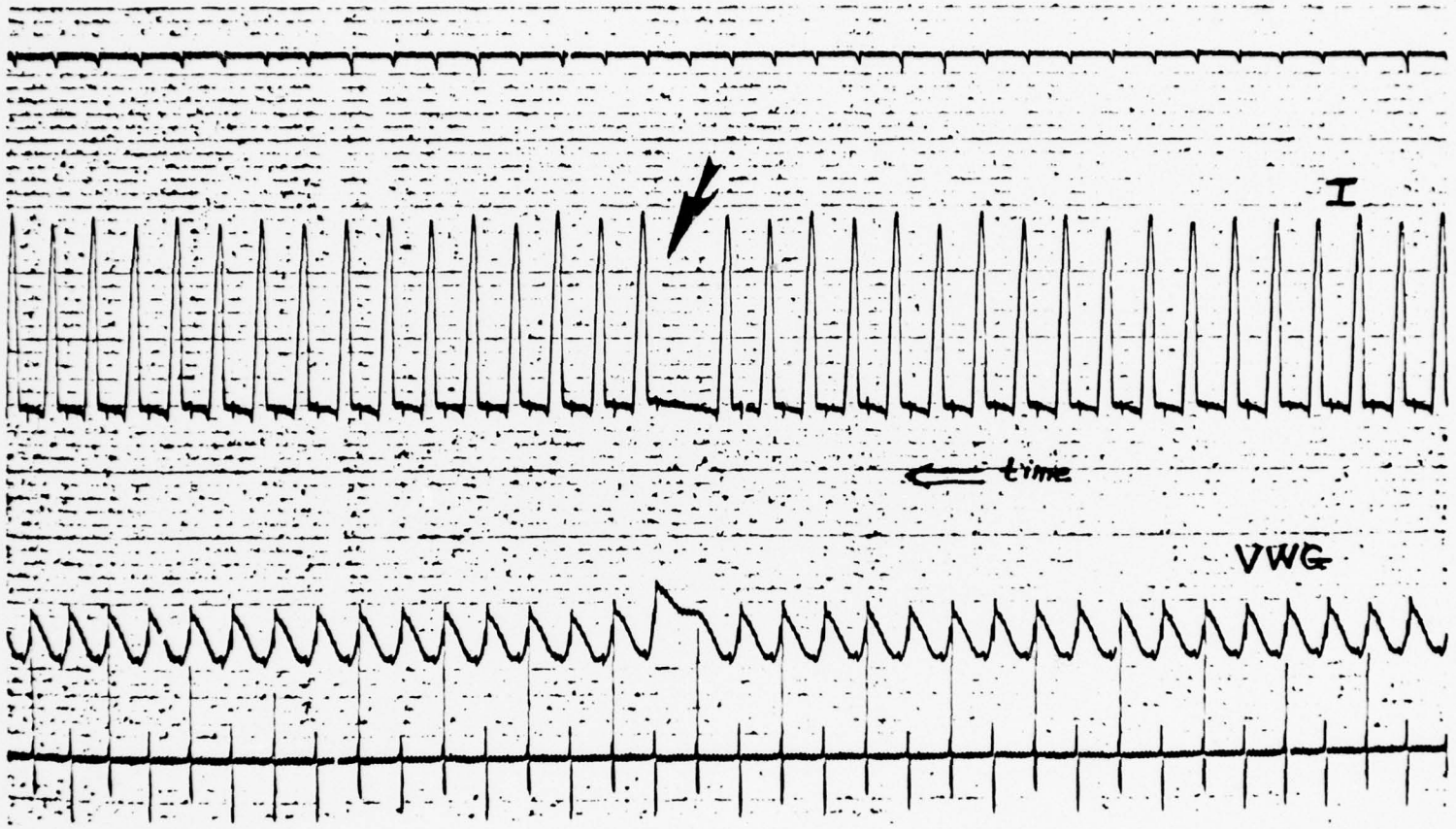

Figure 4-6. Recorded Waveform Several Seconds After Previous Figure. The arror points to a no-fire of both switches. Recharge waveform increased voltage until self break occurred.

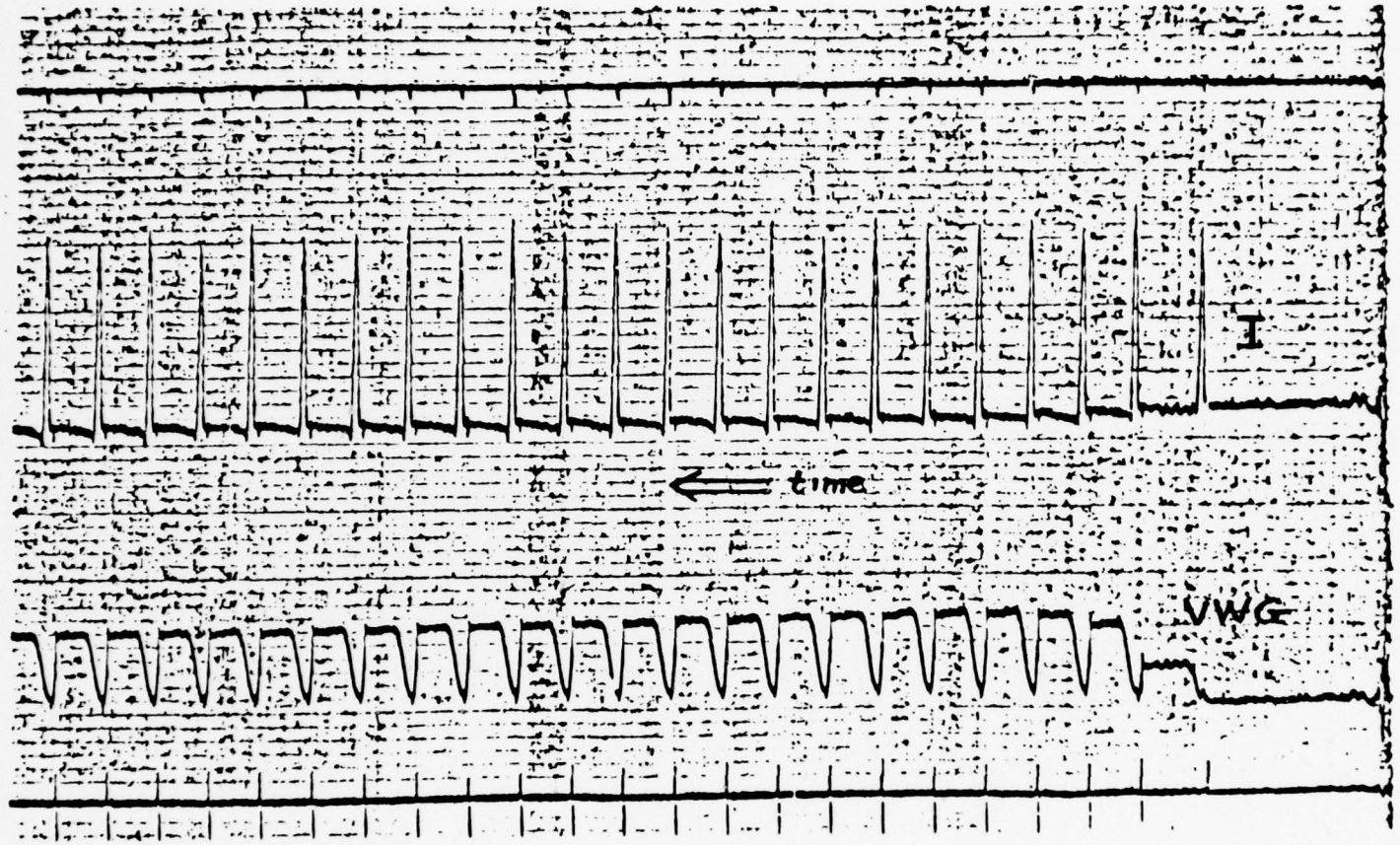

Figure 4-7. Normal Sequence of Recharge and VWG Waveforms at 150 pps.

flow for times of $\lesssim 0.1$ sec before the circuit breaker operates. When this lock-on occurs, hundreds of coulombs flow through the switch, resulting in damage to the electrodes.

Early switch designs (see Progress Report 2) used brass as the active electrode material because of the long lead times for tungsten alloy. Brass was found to become severely pitted from lock-ons. Tungsten alloy was then used as the active electrode material. Figure 4-8 shows switch electrodes which sustained damage and Figure 4-9 shows a typical waveform caused by a lock-on. The tungsten alloy of which the active area of the electrode is composed sustained no apparent damage. However, the arc wandered until the brass parts of this switch were reached and there a degree of damage occurred. The phenomenon of arc wandering is believed caused by the lack of symmetry in the return current which creates magnetic deflection of the arc channel. Occasionally, damage is caused by scortching of the switch envelope which occurs from contact with the channel.

During the recent maximum power and voltage runs, lock-ons were eliminated by the extensive precautions taken to ground and shield the triggering apparatus.

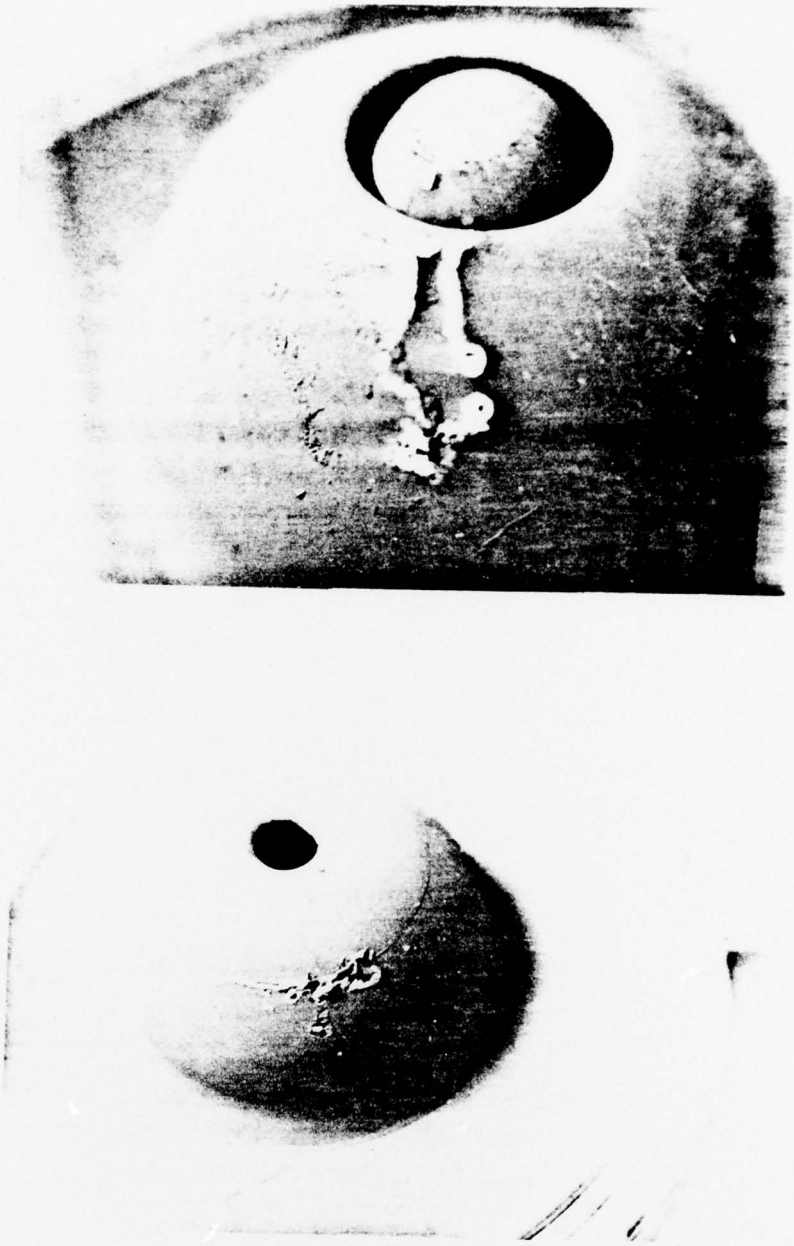

Figure 4-8. Switch Damage Patterns Caused by Lock-ons.

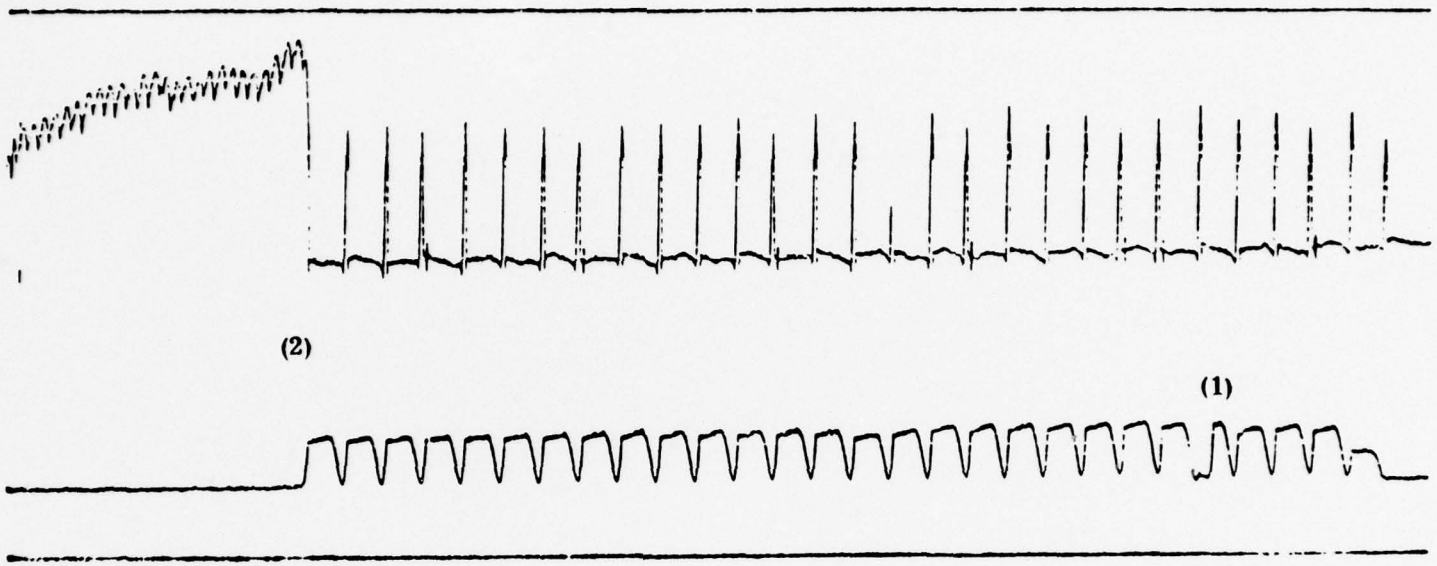

Figure 4-9. Magnetic Tape Record of Recharge Current and VWG Waveform for Early Conf. II Test. Point (1) shows switch prefire, point (2) shows switch lock-on.

APPENDIX I

COMPARISON OF SPARK DISSIPATION IN HIGH-POWER CIRCUIT WITH THAT IN SIMULATOR

This appendix provides a comparison of estimated spark power dissipation in a high-power circuit with that of the simulator circuit used in this program. Energy dissipation in both cases is calculated using Martin's resistive phase formula. This formula provides a means of estimating the time during which a spark descends from infinite impedance down to a resistance equal to the circuit impedance "driving" the spark. In the following approximation we consider the spark resistance constant, at Z_o, and the current constant, at I_o. Initially, the pulse is assumed to end after the duration τ_r, after which time the arc resistance becomes too small to dissipate significant energy.

In a subsequent calculation; we assume an arc-drop of 150 volts is maintained across the arc and compare energy and power dissipation for a pulse of relatively long duration.

The parameters used in the examples correspond to the maximum power level attained during this program.

High-power Circuit

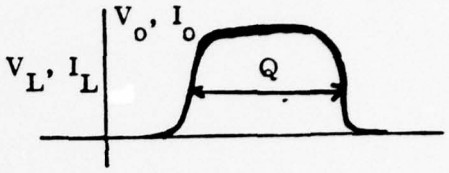

$$W = I^2 Z_o \tau_r = I^2 Z_o \left(\frac{88 \, (\rho/\rho_o)^{1/2}}{Z^{1/3} \, (E)^{4/3}} \right)$$

Example:

V_o = 100 kV

I_o = 5 kA

Q = 240 mC

τ = Q/I = 50 μsec

Z_o = V/I ≃ 20 Ω

ρ/ρ_o = ratio of gas density to atmos. air.

E = gap stress in 10 kV/cm

Z = driving impedance, Ω

d = gap spacing (= 2.0 cm)

$$W = (5 \text{ kA})^2 \, (20 \, \Omega) \left(\frac{88 \, (2)^{1/2}}{20^{1/3} \, (4)^{4/3}} \right)$$

= (500 MW) (7.3 nsec) = 3.7 J

Dissipated power (250 pps) = 3.7 J x 250 = 925 watts

Circuit power (total) = IVτf = 6 MW.

Simulator

$V = 100$ kV

$I_o = 5$ kA

$f = 250$ pps

$Q = 240$ mC

$\tau \simeq 50$ μsec

$$E_g = I^2 Z_o \tau_r = I^2 Z_o \frac{88(\rho/\rho_1)^{1/2}}{Z_o^{1/3} E^{4/3}}$$

Here, gap stress and circuit impedance Z_o differ from that employed in the actual high-power circuit. Obtaining the specified current at a relatively low charge voltage requires a low circuit impedance compared to that of the high-power circuit. Also, the gap stress is lower because in the simulator, the peak voltage serves merely to initiate gap breakdown; the resistive time is determined primarily by the low-voltage, high-current circuit. Therefore, the gap stress is effectively reduced by the ratio of current-source voltage to peak-voltage. Gap spacing and pressure remain the same in both cases, as does the current and total charge transfer.

The calculation therefore goes as follows:

$$Z_o = \sqrt{\frac{L}{C}} = \sqrt{\frac{25\ \mu H}{30\ \mu F}} \simeq 0.9\ \Omega$$

$$E(\text{in } 10 \text{ kV/cm}) = \frac{8 \text{ kV (source voltage)}}{2 \text{ cm (gap)}} \quad \frac{1}{(10 \text{ kV/cm})}$$

$$= 0.4\ (10 \text{ kV/cm})$$

$$E_g = (5 \text{ kA})^2\ (0.9\ \Omega)\ \frac{88\ (2)^{1/2}}{(0.9)^{1/3}\ (0.4)^{4/3}}$$

$$= (22.5 \text{ MW})\ \left(\frac{88 \times 1.41}{0.97 \times 0.30}\right)$$

$$= (22.5 \text{ MW})\ (426 \text{ nsec})$$

This must be considered an upper limit of dissipated energy, based on the assumption the resistive phase is caused solely by the low-voltage source.

$$E_g = 9.6\ J \qquad \text{and} \qquad P_{dis} = 9.6\ J \times 250\ pps = 2.4\ KW$$

Compare dissipated to circuit power:

$$P_{circ} = 1/2\ CV^2 \times 250 = 240\ KW$$

Compare dissipated to simulated power:

$$P_{sim} = VQf = (100\ kV)\ (240\ mC)\ (250\ pps) = 6\ MW$$

Now, compare the "early-time" dissipation which occurs during the resistive time to the "late time" dissipation which occurs due to the arc-drop. T. James and J. L. Browning[(1)] measured arc drop in circuits with parameters comparable to those of interest here. The peak arc drop will be the same in high and low power circuits because the peak currents are the same. The integrated energy which is dissipated in the gas will depend slightly on pulse shape but in this estimate we ignore this difference.

The arc drop for a 2 cm gap under atmospheric pressure is about 150 V. Dissipated power is:

$$W = 5\ kA \times 150\ V \times 50\ \mu sec$$
$$= 38\ J/pulse$$

$$P = 9500\ watts\ for\ a\ 6\ MW\ circuit.$$

The energy dissipated during the early resistive time is much less than that dissipated during the pulse duration. Based on the calculations above, simulating the current for $\approx 50\ \mu sec$ pulses ought to provide the same energy dissipation in the gas, regardless of whether the circuit operates at 6 MW actual or simulated power.

---

(1) Arc Voltage of Pulsed High Current Gaps, T. James and J. L. Browning, U.K.A.E.A. Research Group, Culham Lab. Abingdon, Berks.

APPENDIX II

CALCULATION OF GAS FLOW BASED ON PRESSURE CHANGE OF RESERVOIR

The average gas flow can be estimated using the ideal gas equation. We initially assume temperature is held constant.

$PV = \frac{m}{M} RT$ where P = reservoir pressure

V = reservoir volume = 60 ft^3

m = mass of gas in reservoir

R = gas constant = $8.3 \frac{Joule}{mole\,^\circ K}$

T = absolute temperature

M = mole air $\simeq$ 28 gms

$$m = \frac{MPV}{RT}$$

$$\frac{\overline{dm}}{dt} = \frac{MV}{RT} \frac{dP}{dt}$$

$$\frac{\overline{dm}}{dt} = \frac{MV}{RT} \frac{P_2 - P_1}{\Delta t}$$

$$= \frac{\left(28 \frac{gm}{mole}\right) \times \left(60\ ft^3 \times 0.028 \frac{m^3}{ft^3}\right)}{\left(8.3 \frac{Joule}{mole\,^\circ K}\right) \times (300^\circ K)} \left(\frac{P_2 - P_1}{\Delta t}\right)$$

$$= 1.9 \times 10^{-5} \frac{kg - m^3}{Joule} \left(\frac{P_2 - P_1}{\Delta t}\right)$$

$$P_1 = 100 \text{ psig} = 115 \text{ psia} = 7.8 \times 10^5 \frac{\text{nt}}{\text{m}^2}$$

$$P_2 = 65 \text{ psig} = 80 \text{ psia} = 5.3 \times 10^5 \frac{\text{nt}}{\text{m}^2}$$

$$\frac{P_2 - P_1}{\Delta t} = 1.8 \times 10^5 \frac{\text{nt}}{\text{m}^2} \text{ per minute.}$$

$$\frac{\overline{dm}}{dt} = 1.9 \times 10^{-5} \frac{\text{kg - m}^3}{\text{Joule}} \frac{dP}{dt}$$

$$= \left[1.9 \times 10^{-5} \frac{\text{kg - m}^3}{\text{Joule}}\right] \left(2.5 \times 10^5 \frac{\text{nt}}{\text{m}^2}\right)$$

$$= 4.8 \frac{\text{kg}}{\text{minute}}$$

The gauges are calibrated in SCFM, Standard Cubic Feet per Minute equivalent to 31 g/min.

Therefore

$$\frac{\overline{dm}}{dt} = 155 \text{ SCFM total flow in both switches (77 SCFM per switch)}$$

A temperature drop calculated in Appendix IV occurs in the tank which reduces the pressure about 10%. Increase the final pressure P_2 by 10% to compensate. Then,

$$P_1 = 7.8 \times 10^5 \text{ nt/m}^2$$

$$P_2 = 1.1 \times 5.3 \times 10^5 \text{ nt/m}^2 = 5.8 \text{ nt/m}^2.$$

$$\Delta P/\Delta t = 20 \text{ nt/m}^2 \text{ per min.}$$

$$\frac{d\overline{m}}{dt} = 3.8 \text{ kg/minute} = 123 \text{ SCFM.}$$

$$= 61 \text{ SCFM/swtich.}$$

This is compared to the flow rate obtained from the pitot tube which indicated 1550 feet per minute flowing in a 2-7/8 in. diameter tube. This yields a flow rate of

$$V = vA = \left(1550 \frac{ft}{min}\right) x\ 6.5\ in^2 \left(\frac{ft^2}{144 m^2}\right) = 70 \frac{ft^3}{min}$$

$$= 70\ SCFM$$

Boundary layer correction factor is 0.9. Then, V = 63 SCFM.

This value agrees, within experimental accuracy, with that obtained using the change in reservoir pressure.

APPENDIX III

IMPACT OF RESERVOIR TEMPERATURE CHANGE ON MASS FLOW CALCULATION

Assume adiabatic process: $PV^{\gamma} = \text{const.} = P_o V_o^{\gamma}$. Where γ = ratio of specific heats, $C_p/C_v \simeq 1.4$ for air.

(1) $PV^{\gamma} = P_o V_o^{\gamma}$ $\qquad$ P_o and V_o are initial conditions.

(2) $PV = \frac{m}{M} RT$

From (1) $\quad V = \left(\frac{P_o V_o^{\gamma}}{P}\right)^{1/\gamma}$.

Substitution into (2) yields:

$$P\left[\frac{P_o V_o^{\gamma}}{P}\right]^{1/\gamma} = \frac{mRT}{M} .$$

Simplifying:

$$P^{\frac{\gamma-1}{\gamma}} = \frac{mR}{MV_o} \frac{T}{P_o^{1/\gamma}} = \frac{P_o}{T_o} \frac{T}{P_o^{1/\gamma}}$$

Therefore

$$T = T_o\left(\frac{P}{P_o}\right)^{\frac{\gamma-1}{\gamma}}$$

For $\gamma = 1.4$, $(\gamma-1/\gamma) = 0.29$. For a change in absolute pressure from 115 psia to 80 psia,

$T = \left(\frac{80}{115}\right)^{0.29} T_o = 0.90\, T_o$ which accounts for a 10% reduction in the pressure reading.